Topologies for Satellite Constellations in a Cross-linked Space Backbone Network

by

Jason H. Bau

S. B., Massachusetts Institute of Technology, 2000

Submitted to the Department of Electrical Engineering and Computer Science

in Partial Fulfillment of the Requirements for the Degree of

Master of Engineering in Electrical Engineering and Computer Science

at the

MASSACHUSETTS INSTITUTE OF TECHNOLOGY

May 20, 2002   [June 2002]

Author_____
Department of Electrical Engineering and Computer Science
May 20, 2002

Certified by_____
Vincent W. S. Chan
Joan and Irwin M. Jacob Professor of Electrical Engineering and
Computer Science and Aeronautics and Astronautics
Director, Laboratory for Information and Decision Systems
Thesis Supervisor

Accepted by_____
Arthur C. Smith
Chairman, Department Committee on Graduate Theses

Topologies for Satellite Constellations in a Cross-linked Space Backbone Network

by

Jason H. Bau

Abstract

An evolutionary space data network can be formed from satellites serving as both backbone and user-access nodes connected via high-speed cross-links. Such a space backbone network should support spacecraft-to-ground and spacecraft-to-spacecraft links for users of various altitudes (LEO, MEO, GEO and HEO). One main consideration in the design of such a space network is the physical altitude and topology of the backbone satellite constellation. In this thesis, different GEO, MEO, and LEO configurations are considered as backbone topologies to serve the projected user altitudes and requirements. First, exact constellations are determined for each proposed configuration that meet the user coverage requirements while maximizing coverage efficiency. The complexities of these constellations are then compared using constellation parameters such as altitude, and the number of orbital planes required, and the number of satellites required per plane, as well as individual satellite parameters like the number of antennae required, the necessary slewing rate of each antenna, the power required by each antenna, and the physical placement of these antennae on the satellites. The complexity parameters of each individual satellite will be determined for two of the types of communications links used on the satellite, namely links between the user satellites and backbone satellites and links between backbone satellites. These parameters are then used in a speculative cost model to determine the cost versus complexity of each constellation. Through these calculations, a GEO backbone consisting of three satellites is determined to require a minimum number of apertures for both types of links as well as allowing an optimal onboard placement of these apertures. Thus, it possesses cost vs. complexity characteristics superior to other constellations and should be the choice for a space-borne data backbone network.

Acknowledgements

I would like to express my gratitude to all who supported me during these past two years of graduate school. Many thanks go out to my spiritual leaders Pastor Paul, Becky JDSN, Heechin JDSN and Scott hyung for their constant prayer and concern. I would also like to thank my advisor Professor Chan for his patience and research guidance and my parents for all the years of love and selfless sacrifice they gave to raise me. Thanks also to the Concord brothers, Danny, Walter, Eddie, Austin, Eugene, Patrick, Hero, Matt, and Orton and to the EG brothers, Thomas, Henry, Dave, Alan, and Matt (again) for their love and patience, for putting up with my study habits, and for so many memories. I owe you a great debt of love and a meal or two! My gratitude to all the members of Berkland Baptist Church for being my true spiritual family. It is a privilege for me to be related to you. To my fiancée Amy I am indebted for her constant encouragement and urging to continue my thesis work and for supporting me in innumerable other ways. And finally, to my Savior and my God, without whom I would have neither life nor happiness, I can only express my eternal gratitude and offer my devotion with all of my meager strength. I love you, Lord.

Table of Contents

List of Figures

7

List of Tables

Chapter 1

Introduction and Background

1.1 Motivation

A space backbone network architecture featuring coverage for diverse user orbits and high-rate (>Gbps) user-access and intra-backbone cross-links exhibits desirable traits for supporting spacecraft-ground communications and spacecraft-spacecraft communications. By providing accessibility from a variety of user orbits, such an architecture allows missions of all different purposes and altitudes to send traffic into the same backbone network, where the load can be accommodated by the high capacity intra-backbone cross-links. This allows for a unification and simplification of communications to different missions. Also, a backbone architecture employing cross-links between backbone satellites can eliminate dependency on a widespread network of ground-stations, improving the survivability and security of the system. Additionally, the high capacity cross-links allow the backbone to provide the high-rate spacecraft-to-spacecraft connections necessary to support future applications, such as dedicated orbiting processors that reduce the end-of-life obsolescence of satellites and improve the upgradability of space systems [1]. Thus, given the desirable nature of a space network architecture employing high-rate cross-links and providing coverage for a variety of user orbits, we investigate the design of such a space network.

1.2 Procedure

One of the most fundamental and far-reaching considerations in the design of a space backbone network is the physical placement of the backbone satellite constellation. The primary goal of our backbone constellation is to provide the coverage required by the users. We wish to provide 100% coverage of possible users in LEO, MEO, GEO, and the relevant parts of highly elliptical orbits, as well as support downlinks to a small number of

ground stations inside and outside of the US. These coverage requirements can be met by a variety of constellations, however, each varying in altitude, number of orbits, arrangement of the orbits, and the arrangement of satellites within the orbits. All of these factors will influence the complexity and performance of the overall system. We will quantify the complexity of the system with various parameters, the first of which will be determined by coverage requirements. These will include the constellational parameters of altitude, the number of orbits, the number satellites required per orbit, and the number of ground-stations required. These constellational parameters will determine the complexity of the individual satellites, as each backbone satellite must maintain intra-backbone cross-links within the constellational geometry as well as provide connections for users in its coverage space and downlinks to the earth. Thus, each backbone satellite will require a number of communications apertures, each of which must track a moving target. Thus, the complexity of each individual satellite can be quantified by the number of apertures required, the size required of each aperture, the slewing rate required of each aperture, and any obscuration issues which arise from the placement of apertures on the satellite. We can use these complexity parameters to compare possible backbone system designs with each other. Additionally, these complexity parameters can also be used to drive a speculative cost model based on the communications subsystem of each satellite that can also be used for system comparison. Finally, some network-wide performance measures, such as required backbone link capacity and user blocking probability, can also be derived from the complexity parameters by some limiting assumptions and used for system comparison.

We now proceed to state the assumed user requirements. We will then use the coverage aspect of these requirements to determine several suitable backbone constellations, at which time we will begin a systems comparison of these constellations, beginning with the complexity parameters, then fitting them to a speculative cost model, and finally ending with network-wide performance comparisons.

Chapter 2

Projected User Requirements and Service Contract

2.1 User Requirements

We assume there will be a total of 10-100 data sources circularly orbiting in either low earth orbit (LEO) with altitude from 250 km to 1,500 km, which covers almost all LEO satellites as well as shuttle missions and the ISS, medium earth orbit (MEO) with altitude from 5,000-15,000 km (MEO), geo-synchronous orbit (GEO) at 35,786 km altitude, or highly-elliptical orbit (HEO) with perigee around 1,000 km and apogee around 40,000 km, parameterized as L/M/G/H. We expect two different types of sources. The first sends data via a connection of sizable durations (from minutes to always-on) at rates of 1-100 Gbps, and the second sends short bursts (from fractions of a second to minutes) of 1Mbps to 1Gbps. We also expect that all of the orbiting source spacecraft will sink a small amount of telemetry data but will not model this data because of its low-rate nature. Finally, we make the assumption that source satellites are uniformly distributed in the space of possible user orbits, because they are likely to be earth sensing or observing satellites and thus be evenly distributed to cover the earth.

As for data sinks, we first assume there are 2-4 high-rate network access points on the ground, with 1-2 being fixed in the United States and 1-2 mobile anywhere outside the U.S. There are also up to 10 low-rate (<155Mbps) sink points on the ground and 1-2 sinks in space, in either LEO, MEO, or GEO orbit.

2.2 Services Provided by Backbone Network

Given these user requirement assumptions, the backbone network will provide the following services to the users. The network will provide two classes of connections as mentioned above with a small blocking probability of p_b and will maintain a continuous link once the connection is established. The 10-100 data sources may be in LEO, MEO,

or GEO orbit, within the boundaries listed in table 2-1 for the altitude classes, and may request either class of service. The backbone will also support these data sinks for both types of connection: 1-2 stationary ground stations in the U.S., 1-2 mobile ground stations outside of the U.S., and 1-2 spacecraft in LEO, MEO, or GEO. In addition, the backbone will provide for at most 10 mobile ground sink points for the lower-rate connections. All users will have access to at least one backbone satellite 100% of the time, assuming that access is only limited by visibility, which for the space user is limited only by the blockage of the earth and for the ground user is limited only by a minimum angle of elevation ε. Table 2-1 lists the services provided by the satellite.

Connection Types	Sources	Sinks
Class 1: Long streams of 1-100 Gbps (minutes to always-on)	10-100 total, orbiting in either LEO (30-40 total) (250-1,500 km)	1-2 stationary in U.S. 1-2 mobile outside U.S.
Class 2: Unscheduled access of 1Mbps- 1Gbps bursts (fractions of seconds to minutes)	MEO (20-30 total) (5,000-15,000 km) GEO (30-40 total) (35,786 km)	1-2 total in LEO, MEO, or GEO ~10 mobile Class 2-only access points
Note: Both types of connections available with small blocking probability p_b	Note: All sources and sinks except HEO have visibility to at least 1 backbone satellite 100% of time.	

Table 2-1: Services provided by the backbone network

Chapter 3

Determining Candidate Constellations

3.1 Coverage

We must now determine the satellite constellations that meet the user requirements stated in the previous chapter. Since the solution space of constellations is nearly infinite, we must limit the space of constellations under consideration. First, we choose to limit the altitudes to study. We select only the following orbit altitudes within three altitude classes, GEO at 35,786 km altitude, MEO at 15,000 km, and LEO at 1,500 km. The backbone altitudes for MEO and LEO were selected at the upper boundaries of their altitude classes because we wish to simplify supporting users in the same classes as the backbones. By placing the backbone at the upper boundary of an altitude class, we allow backbone satellites to only look "down" at all potential users within the same class, thus preventing the satellites from having antennas on both their "top" and "bottom" surfaces just to service users within the same class. We thus assume that the altitudes at the upper class boundaries will minimize the user-access complexity and thus also overall system cost.

We also limit the space of constellational arrangements within each altitude to those arrangements that have traditionally been proposed for use with cross-links. The GEO constellation is already well confined, with the only variation being the number of satellites and their locations within the geo-synchronous plane. In the LEO case, we will consider both a constellation of polar orbits and one of inclined Walker orbits, which may be more efficient in the distribution of coverage areas. Finally, in the MEO case, we will

consider both a constellation of polar orbits and a scheme involving several inclined Walker orbits, which may again be more efficient in terms of coverage than the polar configuration. Table 3-1 lists the constellations under consideration in this thesis.

Class	Altitude (km)	Configuration
GEO	35,786	Planar
MEO	15,000 (highest)	Polar
		Walker
LEO	1,500 (highest)	Polar
		Walker
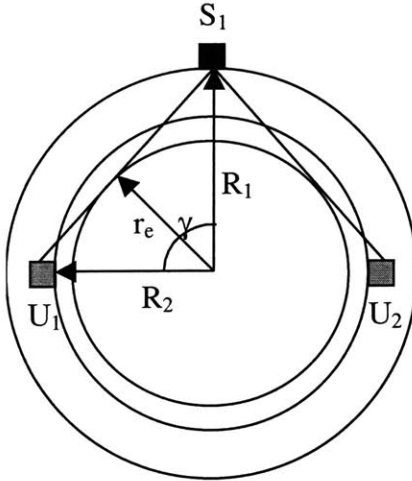
Table 3-1: Backbone constellations under consideration

3.2 Determination of Coverage Radius

Our first goal is to determine where to place individual backbone satellites in order to provide full coverage for all user orbits. The coverage area of each backbone satellite can be limited by obscuration caused by the physical location of the apertures on the satellites, the maximum slewing angle and rate of each aperture and the line-of-sight blockage due to the earth. We will assume that user access links are limited only by the blockage of the earth and determine a constellation based on this condition. Then, we will return to consider to maximum antenna angles and rates to see if these are within the limits of projected technology and also obscuration issue to solve any difficulties these may pose.

The region serviceable by a backbone satellite is any location where its line of sight is not blocked by the earth. Figure 3-1 illustrates this coverage area. We can now use this model for a backbone satellite's service region to determine the number of satellites required for each proposed backbone configuration to provide full coverage for each of the user altitudes. There is a "worst case" user orbit that, if satisfied, would provide service for all of the other user orbits. Because of the earth's obscuration, the minimum angular distance of the radius of the coverage region occurs at the lowest user altitude. Looking at figure 3-1, we can see that if R_2 were decreased while the line between S_1 and

U_1 remains tangent to the earth, γ would also decrease. We can also see that this is true at all backbone altitudes, since a smaller R_2 makes for a smaller γ at any R_1. Thus, for all the backbone altitudes, the minimum coverage radius is determined when servicing the lowest LEO, at 250 km.
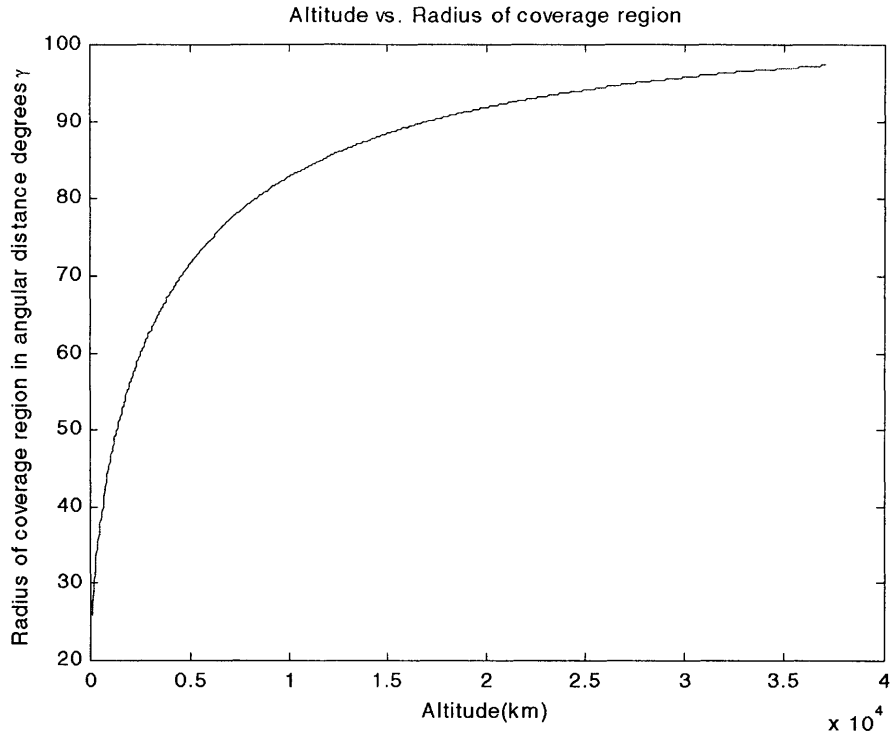
Figure 3-1: An illustration of the coverage region. The coverage region for S_1 is the upper semi-circle between U_1 and U_2. Lines tangent to the earth are drawn from the backbone satellite S_1 to the user satellites S_1 and S_2. R_1 is the backbone orbit radius, and R_2 is the user orbit radius, and r_e is the radius of the earth. γ is radius of coverage region for S_1 on the user orbit sphere in angular distance.

From the figure, we can see that γ can be found from the values of R_1 and R_2. With some trigonometry, we find that this relationship is

$$\gamma = \cos^{-1}\left(\frac{r_e}{R_1}\right) + \cos^{-1}\left(\frac{r_e}{R_2}\right) \tag{3.1}$$

Fixing $R_1 = r_e + 250$, we can compute γ as a function of R_2, the backbone orbit altitude. This is plotted below in figure 3-2.

17

Altitude vs. Radius of coverage region
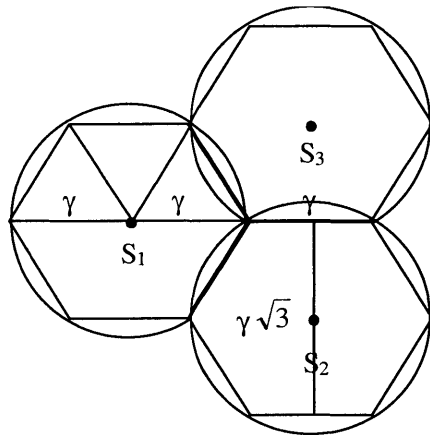
Figure 3-2:   The altitude of the backbone satellite vs. the radius in angular distance of the coverage region for a 250km circular orbit

For our critical altitudes of 1500 km, 15,000 km, and 35,786 km, the radius of the coverage region corresponds to 51.7°, 88.4°, and 97.1°.

3.3 Polar Orbits

For polar orbits, the number of satellites required for full coverage of the user sphere can be calculated in the following way. We first define satellites in adjacent planes to orbit in the same direction, except across two seams where there are retrograde adjacent planes. We also require that when a satellite in a particular plane is over the equator, the midpoint of the nearest satellites in the closest eastward plane is also over the equator. Because the individual orbits or a polar configuration are furthest from each other over the earth's equator, we can use coverage at the equator to determine the number of orbital planes necessary in the constellation. Looking at figure 3-3, we can see that each orbital plane covers 2γ of angular distance in its ascending direction. In

descending direction, each orbital plane will cover only γ of angular distance, because of its phasing.

Figure 3-3: An illustration for the calculation of the number of satellites required for a polar orbit to provide coverage for the full user sphere. The meeting of three satellites is shown here, with S_1 being on the equator of the user sphere.

Thus, the total number of orbital planes required to cover the equator is
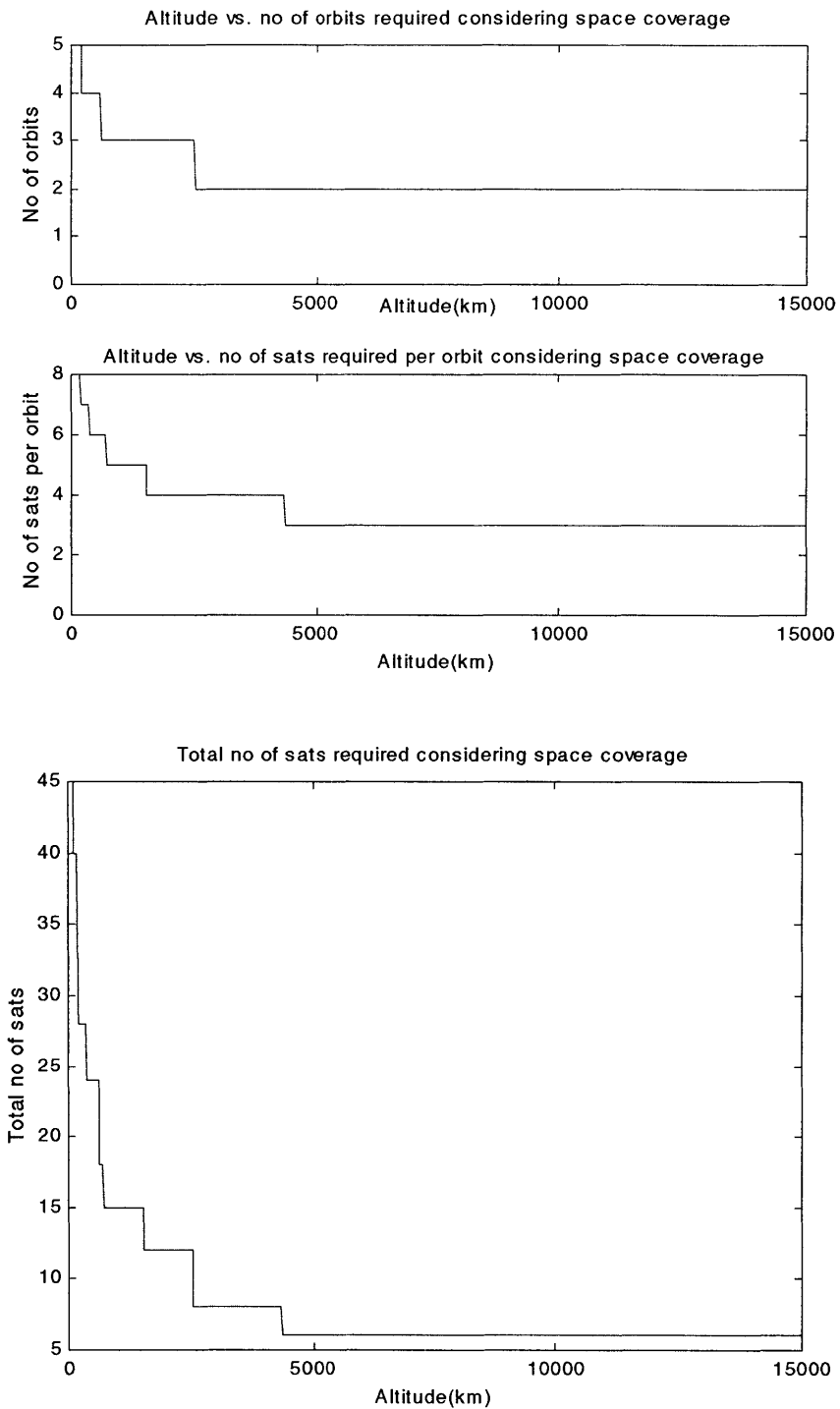
$$P = \left\lceil \frac{360}{3\gamma} \right\rceil \tag{3.2}$$

Looking at the same figure, we can see that the total number of satellites required to cover all of one orbital plane is

$$S = \left\lceil \frac{360}{\sqrt{3}\gamma} \right\rceil \tag{3.3}$$
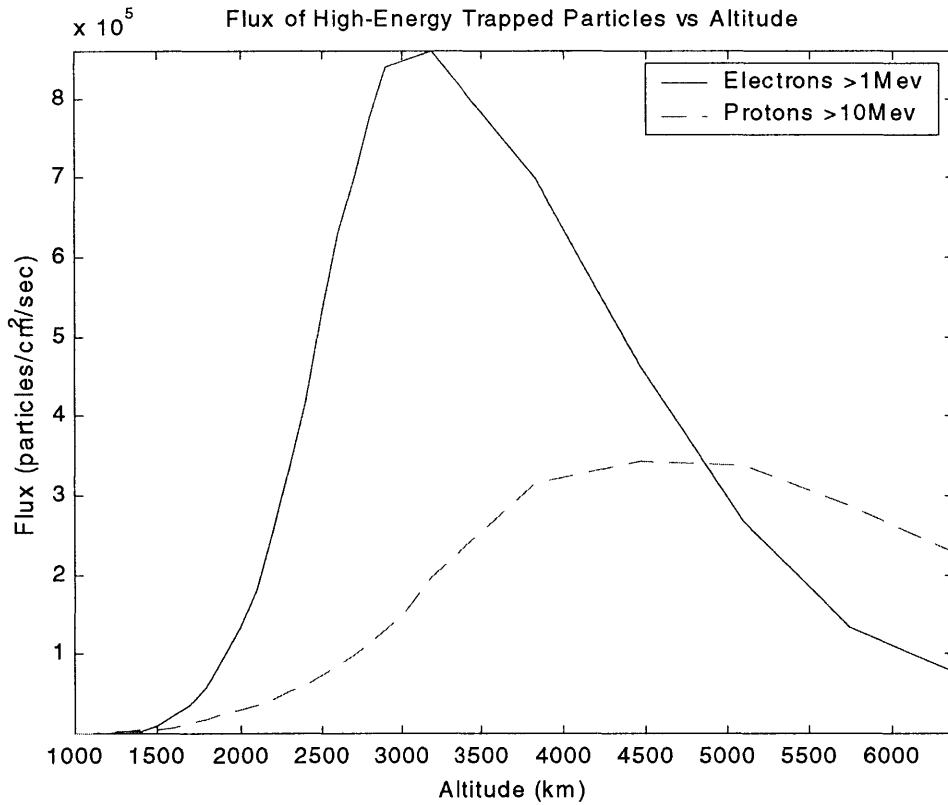
Thus the total number of satellites required to provide full coverage of the user sphere is T = P*S.

We have plotted the values of S, P, and T versus altitude for a polar configuration. These are shown in figure 3-4.

19

Figure 3-4: The number of orbital planes, satellites per plane, and total satellites required for full coverage of the 250 km user sphere under the polar configuration as a function of altitude.

We can see that T is 6 at 15,000 km and 12 at 1,520 km. The graph for T breaks from 15 to 12 at 1,520 km altitude, whose difference from 1,500 km is negligible. We could also try to reduce T by placing the altitude at the next break point, which is at 2,500 km. This places the backbone satellites squarely at in the inner Van Allen belt, however, so much more radiation shielding would be required. According the NASA's AE-8 and AP-8 trapped radiation models[1], which give predictions for proton and electron flux at various altitudes, the flux of high energy protons (>10Mev) that could damage the spacecraft during solar maximum conditions increases by an order of magnitude from 1,500km to 2,500km. The flux of high energy electrons (>1Mev) increases 50-fold. These results are summarized figure 3-5. Thus, it is not advantageous to move the backbone up to 2,500 km in order to reduce the number of required satellites.
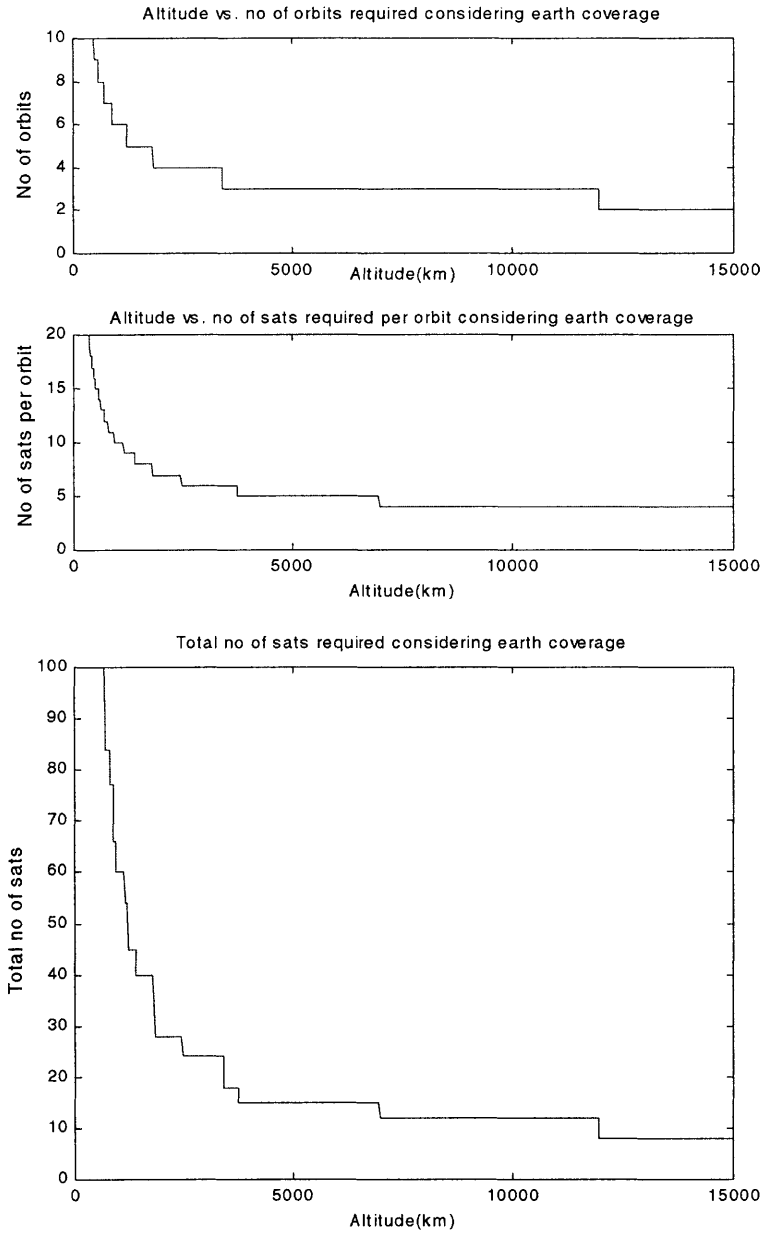
Figure 3-5: The fluxes of high-energy electrons and protons in the inner Van Allen belt during solar maximum. The fluxes occur over the equatorial plane and are time-averages. Data points taken from NASA's AE8max and AP8max models [4].

Thus far, we have determined that for polar orbits at 1,500km, 3 orbital planes with 4 satellites per plane to provide coverage to all space user orbits. We have not considered how this orbit will cover the earth, however. Given a minimum angle of elevation requirement ε, the angular distance of the radius of terrestrial coverage region, γ_e, can be determined as a function of backbone orbit radius R_2. This equation is determined by Walker [2] as

$$\gamma_e = \cos^{-1}\left(\frac{r_e \cos(\varepsilon)}{R_2}\right) - \varepsilon. \tag{3.4}$$

Thus, when γ_e is used in the equations for P and S, we obtain the following plots

Figure 3-6: The number of orbits, satellites per orbit, and total satellites required for full terrestrial coverage in a polar configuration as a function of altitude.

At 1,500 km, P is 5 and S is 8 when the γ_e with $\varepsilon=10°$ is used instead of γ. This implies that the minimum configuration which satisfies coverage requirements for space users, at P = 3 and S = 4, does provide full global coverage. Thus, multiple ground-stations must be used in order to provide continuous downlink availability.

For the MEO constellation, there is only a two satellite difference, resulting from S=4 for the full ground coverage case and S=3 for the orbital coverage case, between

constellations providing full ground coverage and full orbital coverage. Thus, we expect that any gaps in ground coverage will occur between satellites in the same orbit. Thus, we may be able to place two ground-stations separated by a few degrees in latitude to provide continuous downlink availability. The results for the polar orbits are summarized in table 3-2.

Type of Coverage	Full Orbital Coverage			Full Ground Coverage		
Parameter	No. of Orbits	No. of Sats/Orbit	No. of Sats	No. of Orbits	No. of Sats/Orbit	No. of Sats
LEO (~1,500 km)	3	4	12	5	8	40
MEO (~15,000 km)	2	3	6	2	4	8

Table 3-2: Summary of polar constellations providing full coverage for users

3.4 GEO Orbit

It is a well-known fact that 3 evenly spaced GEO satellites can provide full terrestrial coverage except in polar regions. We consider whether this is the case for user orbits. The angular radius of the coverage region for GEO backbone satellites in the limiting user orbit sphere (250 km radius) was previously calculated to be 97.1°. Placing two such spherical circles with centers directly opposite each other on the equator of a sphere will cover all of the sphere, even including polar regions, since a circle with angular radius 90° represents exactly half of the sphere. Thus, we can proceed knowing that any evenly distributed GEO constellation with two or more satellites will provide full coverage of all of the user orbits, and any GEO constellation with at least 3 satellites will cover all of the earth as well.

3.5 Walker LEO and MEO orbits

A previous computational study by Walker [3] has been performed to determine the number of satellites in a Walker configuration required to provide full coverage of a sphere. The critical factor in determining whether a constellation meets full coverage requirements is whether the furthest angular distance from any point on the sphere to the

nearest sub-satellite point over one orbital period, R_{Max}, exceeds the radius of the coverage region, γ. If this is the case, then global coverage requirements are not met. Walker's study minimized R_{Max} for each value of T, the number of satellites in the constellation, over "delta" constellations of parameterized by T/P/δ/F, where T is the total number of satellites, P is the number of orbital planes with ascending nodes evenly spaced around a reference plane (usually the equatorial plane), δ is the inclination of each plane with respect to the reference plane, and F is a phasing parameter such that when a satellite is at its ascending node, there is a satellite in the plane with the nearest easterly ascending node which has passed 360•F/T degrees past its ascending node. The study discovered a 10-satellite constellation with the parameters of 10/5/57.1°/2 which has minimum R_{max}=52.2°. This corresponds to the coverage region provided by an altitude of 1548 km, which is before the radiation effects become severe. Thus, this constellation provides coverage for the entire 250-km altitude sphere and is a suitable constellation for study in the LEO orbit.

For the MEO altitude, γ = 88.4°, which is nearly 90°. Thus, we know that by placing 2 satellites directly opposite each other in the same orbital plane, we will already have covered nearly all of the entire 250-km altitude user sphere. Walker's study suggests that a 5/5/60.9°/1 delta constellation will provide full coverage. We can also expect that a 4/2/45°/1 constellation will provide a very high level of coverage (~99.5%) while saving one satellite and three orbital planes. Thus, this is also a suitable constellation for study. The constellations to be included in this study are listed in table 3-3.

	Altitude (km)	Total no of Sats (T)	No of Orbital Planes (P)	No of Sats per Plane (S)	Inclination of Planes (δ)	Phasing Parameter (F)
Polar LEO Space	1,550	12	3	4	90°	1.5
Polar LEO Earth	1,550	40	5	8	90°	2.5
Walker LEO	1,550	10	5	2	57.1°	2
Polar MEO Space	15,000	6	2	3	90°	1
Polar MEO Earth	15,000	8	2	4	90°	1
Walker MEO 1	15,000	5	5	1	43.7°	1
Walker MEO 2[1]	15,000	4	2	2	45°	1
GEO	35,786	3	1	3	0°	N/A
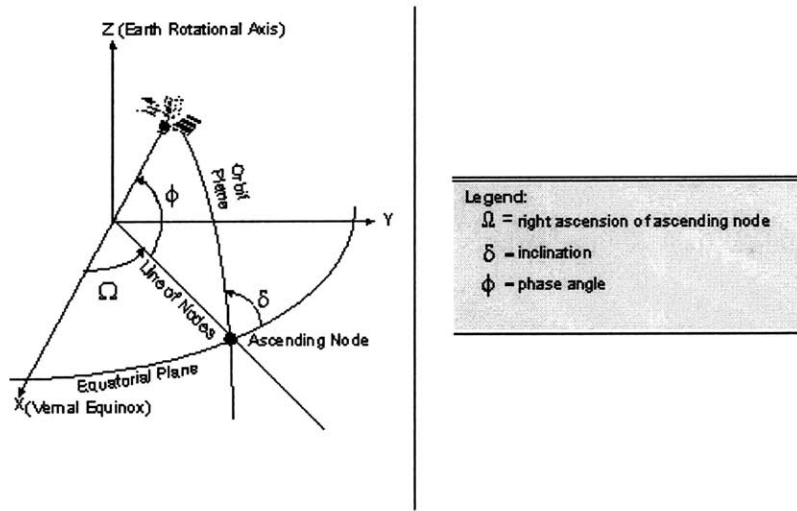
[1]This constellation does not provide 100% coverage of the lowest LEO user altitude. It does provide a very high level of coverage (~99.5%) and is thus included.

Table 3-3: The constellations under consideration in the study. All provide 100% coverage of all user orbits except where noted.

Chapter 4

Complexity of Backbone Links

Since the exact constellations have been determined, the next step is to discover the complexity of the communications links of the individual satellites in each configuration. The first are the intra-backbone links, followed by the user-access links and the space-to-ground downlinks. We first examine the distance and pointing angle variation of intra-backbone links over an orbital period. Consider the diagram of circular orbital geometry in figure 4-1 below. The position of a satellite can be defined in terms of the altitude plus three orbital parameters, Ω, the right ascension of the ascending node, δ, the inclination of the orbit, and ϕ, the phase angle. We also know from Kepler's laws that ϕ is a linear function of time. Thus, if we can define satellite position in terms of ϕ, then we can measure link distance and pointing angle variation as a function of time.

Figure 4-1: Orbital Geometry. Source: Satellite Toolkit Software by Analytical Graphics, Inc [5].

After some calculation, we can find the Cartesian position (x,y,z) of the satellite as a function of Ω, δ, and ϕ. The equation is

$$x = R_1(\cos\phi\cos\Omega - \sin\phi\cos\delta\sin\Omega)$$
$$y = R_1(\cos\phi\sin\Omega + \sin\phi\cos\delta\cos\Omega) \qquad (4.1)$$
$$z = R_1(\sin\phi\sin\delta)$$

where R_1 is the radius of the backbone satellite orbit.

4.1 Inter-Plane Links

4.1.1 Polar Orbits

We now consider a backbone link in the simplest case, which is the polar case. Intra-plane links have a fixed distance and angle, so we first consider inter-plane links. First, we set $\delta = 90°$. Next, we consider a cross-link from a reference satellite in the orbit with $\Omega = 0°$ to the nearest satellite in the next plane to the east, which has $\Omega = \Omega_c = 360/(2*P)$. This satellite has phase angle $\phi_c = 360/(2*S)$ when the reference satellite is at its ascending node. The Cartesian coordinates of the reference satellite can be defined as a vector in terms of ϕ as

$$\mathbf{s_1} = \begin{bmatrix} x_1 \\ y_1 \\ z_1 \end{bmatrix} = \begin{bmatrix} R_1\cos\phi \\ 0 \\ R_1\sin\phi \end{bmatrix}. \qquad (4.2)$$

The coordinates of the second satellite have the equation

$$\mathbf{s_2} = \begin{bmatrix} x_2 \\ y_2 \\ z_2 \end{bmatrix} = \begin{bmatrix} R_1\cos(\phi+\phi_c)\cos(\Omega_c) \\ R_1\cos(\phi+\phi_c)\sin(\Omega_c) \\ R_1\sin(\phi+\phi_c) \end{bmatrix}. \qquad (4.3)$$

Thus we can find the distance variation in terms of ϕ as

$$\mathrm{d}^2 = \|\mathbf{s_2}-\mathbf{s_1}\|^2. \qquad (4.4)$$

In order to find the variation in pointing angle as a function of ϕ, we must first place the link vector $(\mathbf{s_2}-\mathbf{s_1})$ into the frame of the reference satellite. We define the frame as follows: the direction x' is the direction of the velocity vector of the reference satellite; the direction z' points from the satellite away from the center of the earth; and the direction y' points in the direction which satisfies the right hand rule that $\hat{\mathbf{x}}'\times\hat{\mathbf{y}}' = \hat{\mathbf{z}}'$. The unit vectors are as follows

$$\hat{x}' = \begin{bmatrix} \hat{x} & \hat{y} & \hat{z} \end{bmatrix} \begin{bmatrix} -\sin\phi \\ 0 \\ \cos\phi \end{bmatrix}, \; \hat{y}' = \begin{bmatrix} \hat{x} & \hat{y} & \hat{z} \end{bmatrix} \begin{bmatrix} 0 \\ -1 \\ 0 \end{bmatrix}, \; \hat{z}' = \begin{bmatrix} \cos\phi \\ 0 \\ \sin\phi \end{bmatrix} \begin{bmatrix} \hat{x} & \hat{y} & \hat{z} \end{bmatrix}. \quad (4.5)$$

The link vector $(s_2 - s_1)$ in the new coordinate system is

$$\left((s_2 - s_1) \bullet \hat{x}' \right)\hat{x}' + \left((s_2 - s_1) \bullet \hat{y}' \right)\hat{y}' + \left((s_2 - s_1) \bullet \hat{z}' \right)\hat{z}' . \quad (4.6)$$

The elevation angle of the link, λ, which is the angle the link vector makes with the plane formed by $\hat{x}'$ and $\hat{y}'$, has the equation

$$\lambda = \tan^{-1}\left(\frac{(s_2 - s_1) \bullet \hat{x}'}{\sqrt{\left((s_2 - s_1) \bullet \hat{y}' \right)^2 + \left((s_2 - s_1) \bullet \hat{z}' \right)^2}} \right) \quad (4.7)$$
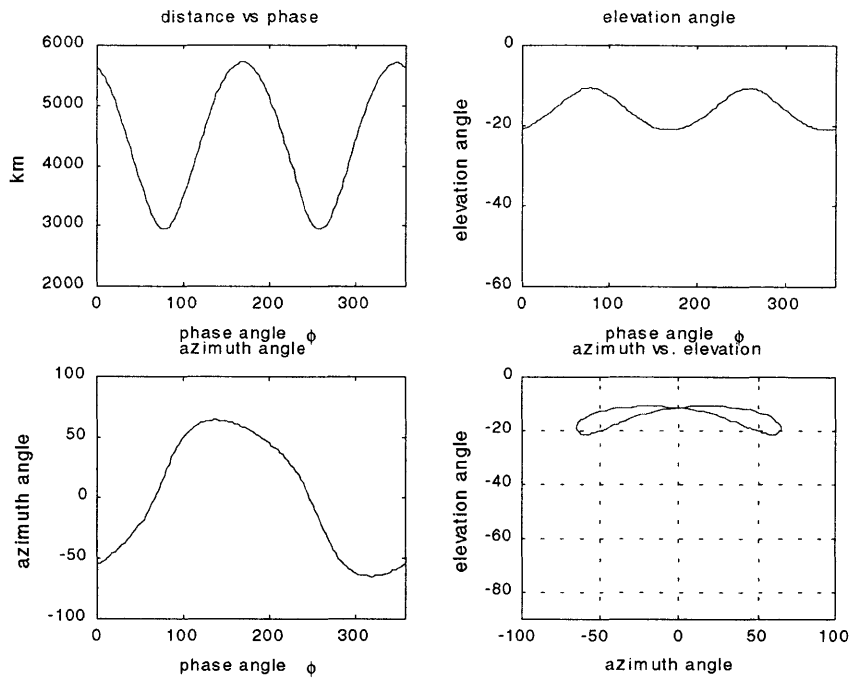
and the azimuth angle of the link, α, which is the angle the link vector makes with the plane formed by $\hat{x}'$ and $\hat{z}'$, has the equation

$$\alpha = \tan^{-1}\left(\frac{(s_2 - s_1) \bullet \hat{y}'}{(s_2 - s_1) \bullet \hat{x}'} \right). \quad (4.8)$$

We now plot the variation in distance, elevation angle, azimuth angle, and combined pointing angle for all of our polar configurations.
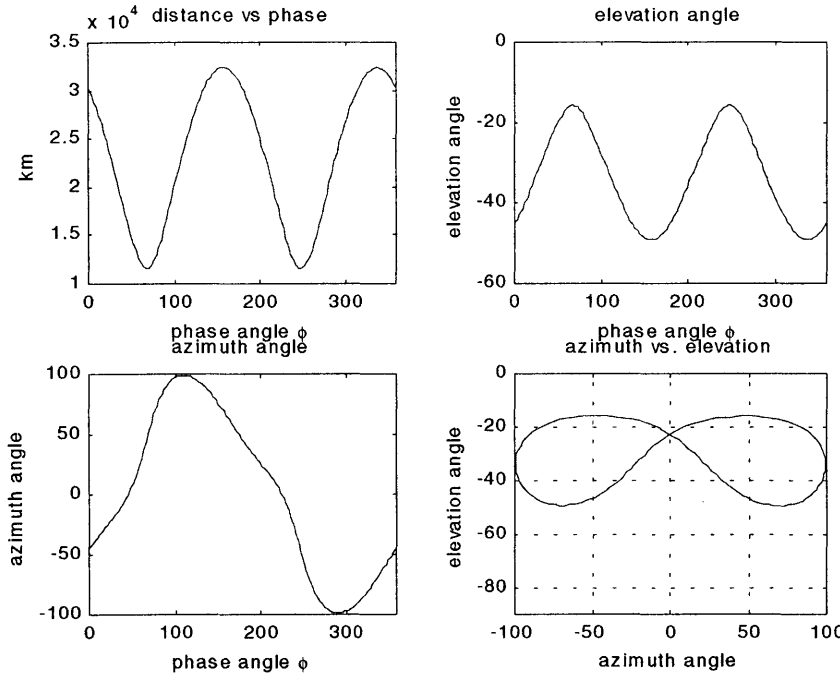
Figure 4-2: Inter-plane cross-link parameter variations vs. phase angle for P = 3, S = 4, and altitude = 1,550

29

Figure 4-3: Inter-plane cross-link parameter variations vs. phase angle for P = 5, S = 8, and altitude = 1,550

Figure 4-4: Inter-plane cross-link parameter variations vs. phase angle for P = 2, S = 3, and altitude = 15,000

x 10^4 distance vs phase

km

phase angle φ

elevation angle

elevation angle

phase angle φ

azimuth angle

azimuth angle

phase angle φ

azimuth vs. elevation

elevation angle

azimuth angle

Figure 4-5: Inter-plane cross-link parameter variations vs. phase angle for P = 2, S = 4, and altitude = 15,000

4.1.2 Walker Orbits

We now generalize the equations for distance and angle variation for the inter-plane cross-link from polar orbits into the inclined orbits used by Walker constellations. Once again, we first describe the orbit of a reference satellite which has right ascension Ω = 0° and consider its cross-link to the nearest satellite in the plane with the nearest easterly ascending node, which has $\Omega = \Omega_c = 360°/2/P$. When the reference satellite is at its ascending node, the nearest satellites in the easterly direction have phase angles ϕ_{c1} = 360°*F/T and ϕ_{c2} = -360°*(P-F)/T. The position of the reference satellite can be described in Cartesian coordinates as

$$\mathbf{s}_1 = \begin{bmatrix} x_1 \\ y_1 \\ z_1 \end{bmatrix} = R_1 \begin{bmatrix} \cos\phi \\ \sin\phi\cos\delta \\ \sin\phi\sin\delta \end{bmatrix} \tag{4.9}$$

and the position of the other satellite can be described as

31

$$\mathbf{s_2} = \begin{bmatrix} x_2 \\ y_2 \\ z_2 \end{bmatrix} = R_1 \begin{bmatrix} \cos(\phi + \phi_c)\cos\Omega_c - \sin(\phi + \phi_c)\cos\delta\sin\Omega_c \\ \cos(\phi + \phi_c)\sin\Omega_c + \sin(\phi + \phi_c)\cos\delta\cos\Omega_c \\ \sin(\phi + \phi_c)\sin\delta \end{bmatrix}. \tag{4.10}$$

As δ, Ω_c, and ϕ_c are fixed, we can see that these position vectors are functions of ϕ, the phase angle. Given these equations, we can calculate the distance variation between the satellites, d, as

$$d^2 = \|\mathbf{s_2} - \mathbf{s_1}\|^2. \tag{4.11}$$

Moving on to the variation of the pointing angle, we must again find the link vector ($\mathbf{s_2} - \mathbf{s_1}$) in the coordinate frame of the reference satellite. As before, the x' direction of this frame points in the same direction as the velocity vector of the satellites, the z' direction of this frame points away from the center of the earth, and the direction y' points in the direction which satisfies the right hand rule that $\hat{x}' \times \hat{y}' = \hat{z}'$. For Walker orbits, however, the reference satellite travels in a plane inclined by an arbitrary amount δ instead of a fixed 90°. In this configuration, the unit basis of the coordinate system of this satellite, as described above, is

$$\hat{x}' = \begin{bmatrix} \hat{x} & \hat{y} & \hat{z} \end{bmatrix} \begin{bmatrix} -\sin\phi \\ \cos\phi\cos\delta \\ \cos\phi\sin\delta \end{bmatrix}, \quad \hat{y}' = \begin{bmatrix} \hat{x} & \hat{y} & \hat{z} \end{bmatrix} \begin{bmatrix} 0 \\ -\sin\delta \\ \cos\delta \end{bmatrix}, \quad \hat{z}' = \begin{bmatrix} \hat{x} & \hat{y} & \hat{z} \end{bmatrix} \begin{bmatrix} \cos\phi \\ \sin\phi\cos\delta \\ \sin\phi\sin\delta \end{bmatrix} \tag{4.12}$$
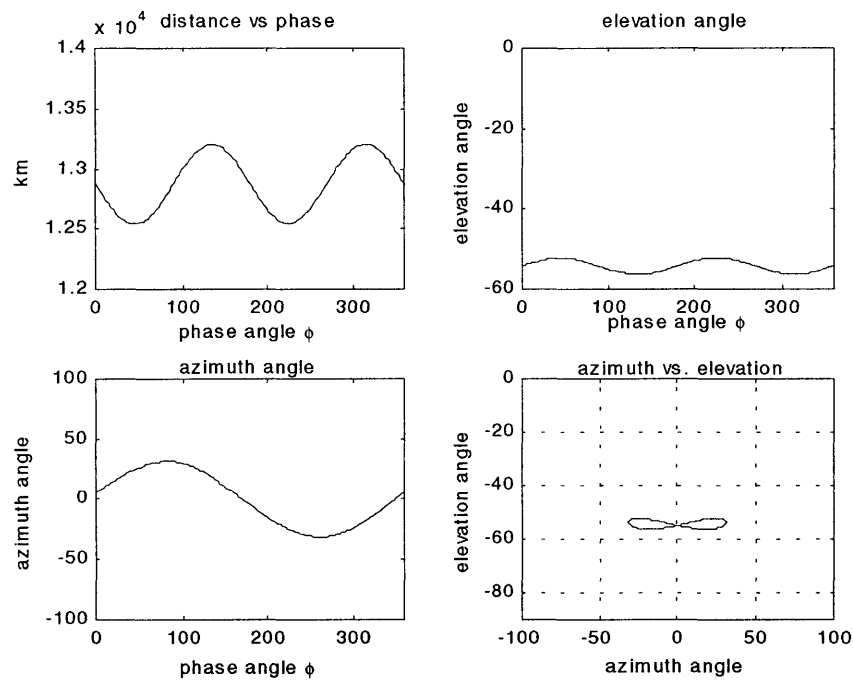
As a sanity check, we see that if we set $\delta = 90°$, we obtain an equation for the basis of the polar configuration which is equal to equation (4.5). Equation (4.7) is still applicable for the elevation angle variation with respect to phase angle, while equation (4.8) can be used for the azimuth angle. Once again, the elevation angle of the link, λ, which is the angle the link vector makes with the plane formed by $\hat{x}'$ and $\hat{y}'$, has the equation

$$\lambda = \tan^{-1}\left(\frac{(\mathbf{s_2} - \mathbf{s_1}) \bullet \hat{x}'}{\sqrt{((\mathbf{s_2} - \mathbf{s_1}) \bullet \hat{y}')^2 + ((\mathbf{s_2} - \mathbf{s_1}) \bullet \hat{z}')^2}} \right) \tag{4.7}$$
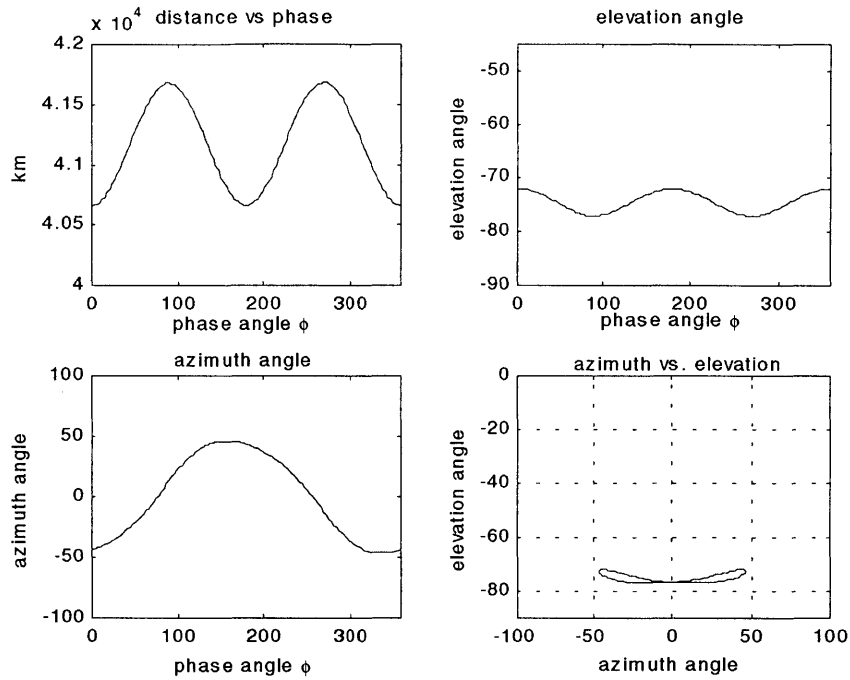
and the azimuth angle of the link, α, which is the angle the link vector makes with the plane formed by $\hat{x}'$ and $\hat{z}'$, has the equation

$$\alpha = \tan^{-1}\left(\frac{(\mathbf{s_2} - \mathbf{s_1}) \bullet \hat{y}'}{(\mathbf{s_2} - \mathbf{s_1}) \bullet \hat{x}'} \right). \tag{4.8}$$

We now plot the variation in distance, elevation angle, azimuth angle, and combined pointing angle for all of our Walker configurations.

Figure 4-6: Inter-plane cross-link parameter variations vs. phase angle for Walker configuration 10/5/57.1°/2, and altitude = 1,550.

Figure 4-7: Inter-plane cross-link parameter variations vs. phase angle for Walker configuration 5/5/43.7°/1, and altitude = 15,000.

Figure 4-8: Inter-plane cross-link parameter variations vs. phase angle for Walker configuration 4/2/45°/1, and altitude = 15,000.
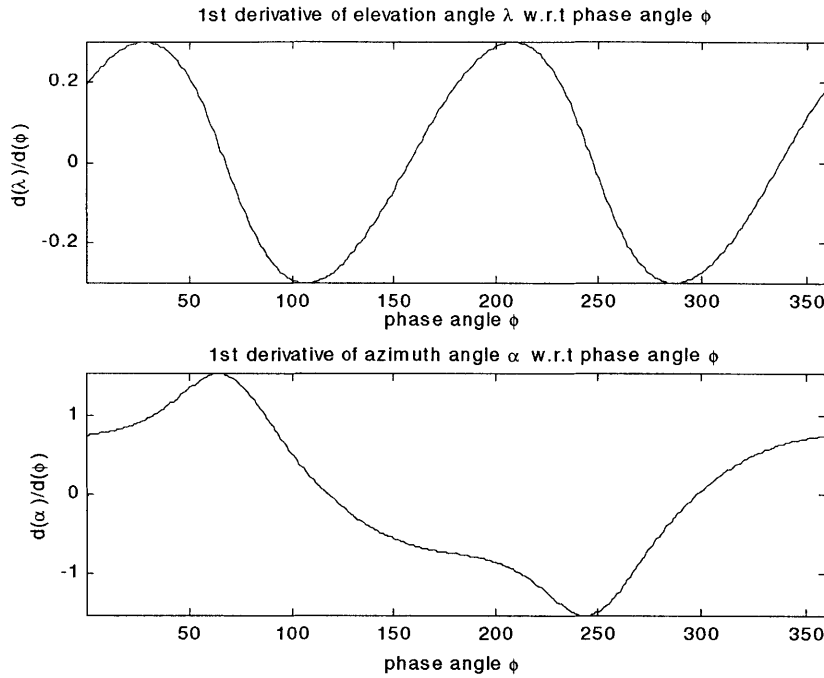
The maximum range, maximum azimuth angle, and the difference between the maximum and minimum elevation angles for an inter-plane cross-link are listed below for the seven LEO and MEO constellations.

	Altitude (km)	Walker Designation T/P/F	Inclination of Planes (δ)	Max Range (km)	Max Azimuth Angle (°)	Δ of Max and Min Elevation Angle (°)
Polar LEO Space	1,550	12/3/1.5	90°	9,511	71.0	-17.5
Polar LEO Earth	1,550	40/5/2.5	90°	5,715	64.7	-10.4
Walker LEO	1,550	10/5/2	57.1°	13,202	31.7	-4.07
Polar MEO Space	15,000	6/2/1	90°	33,801	94.0	-31.5
Polar MEO Earth	15,000	8/2/1	90°	32,371	99.0	-33.5
Walker MEO 1	15,000	5/5/1	43.7°	41,675	46.4	-5.09
Walker MEO 2	15,000	2/2/1	45°	42,344	90.0	-23.0
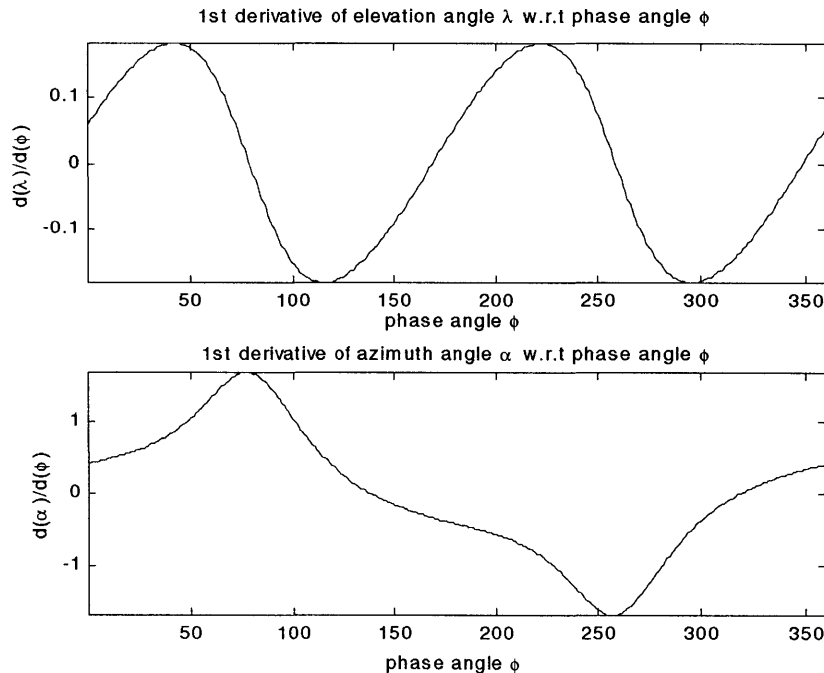
Table 4-1: A summary of intra-backbone links for LEO and MEO constellations.

4.1.3 Slewing Rate
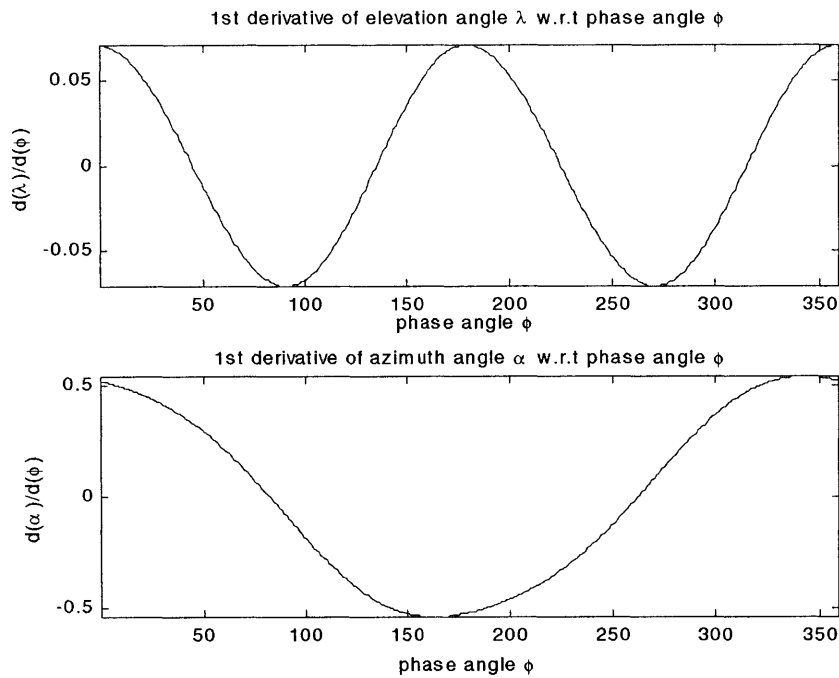
The slewing rates required of the backbone-link apertures are another set of parameters to be determined in characterizing the complexity of the intra-backbone link. These rates can be determined by taking the first derivatives of the variations of elevation- and azimuth-angle with respect to phase angle, which is directly proportional to time. To perform this study, equations (4.7) and (4.8) were differentiated with respect to ϕ for all polar and Walker constellations and the resulting $d\lambda/d\phi$ and $d\alpha/d\phi$ plotted. The resulting graphs and a summary table follow.
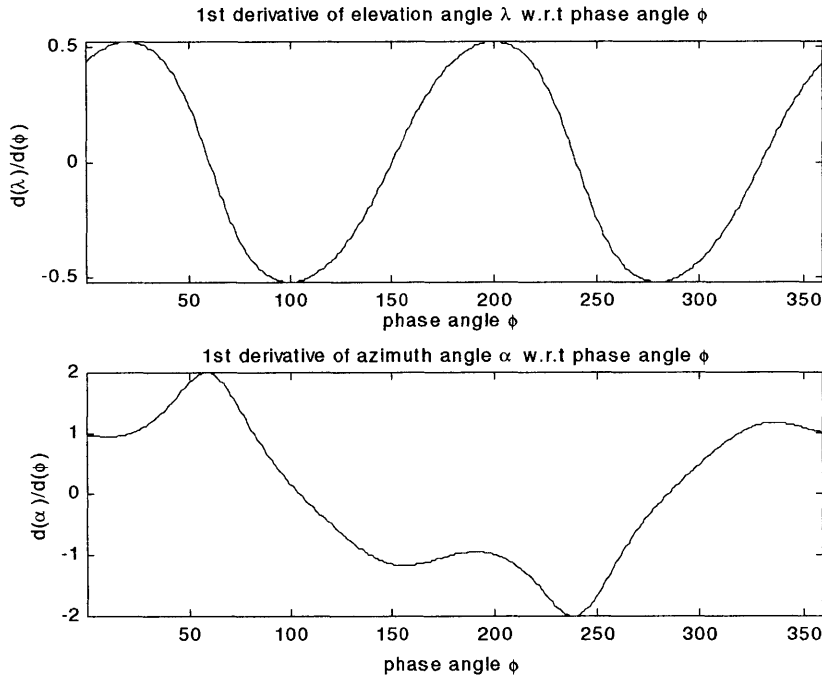
Figure 4-9: The 1st derivatives of the elevation and azimuth angles with respect to phase angle for the polar configuration P=3, S=4, and altitude = 1,550 km.
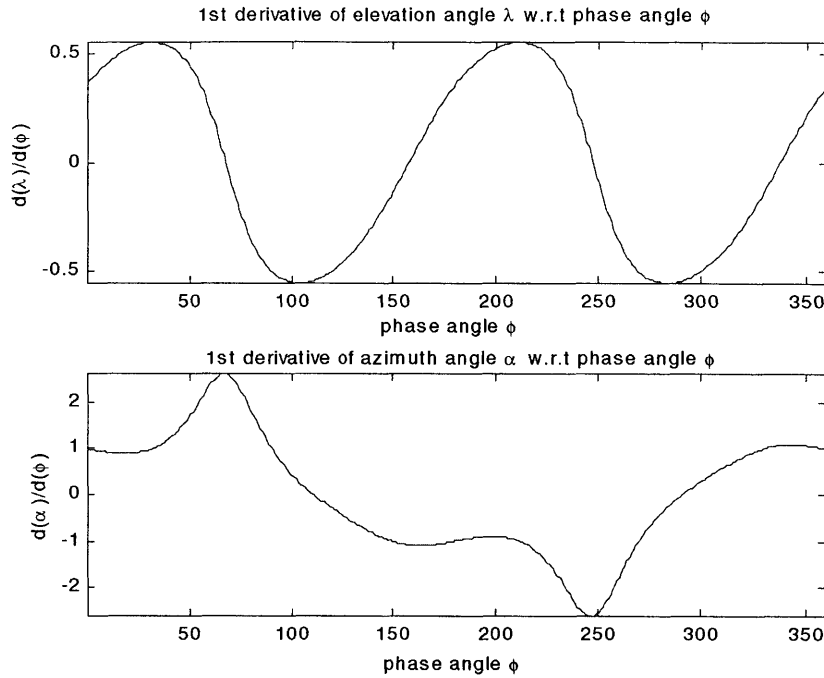
Figure 4-10: The 1st derivatives of the elevation and azimuth angles with respect to phase angle for the polar configuration P=5, S=8, and altitude = 1,550 km.

1st derivative of elevation angle λ w.r.t phase angle φ

1st derivative of azimuth angle α w.r.t phase angle φ
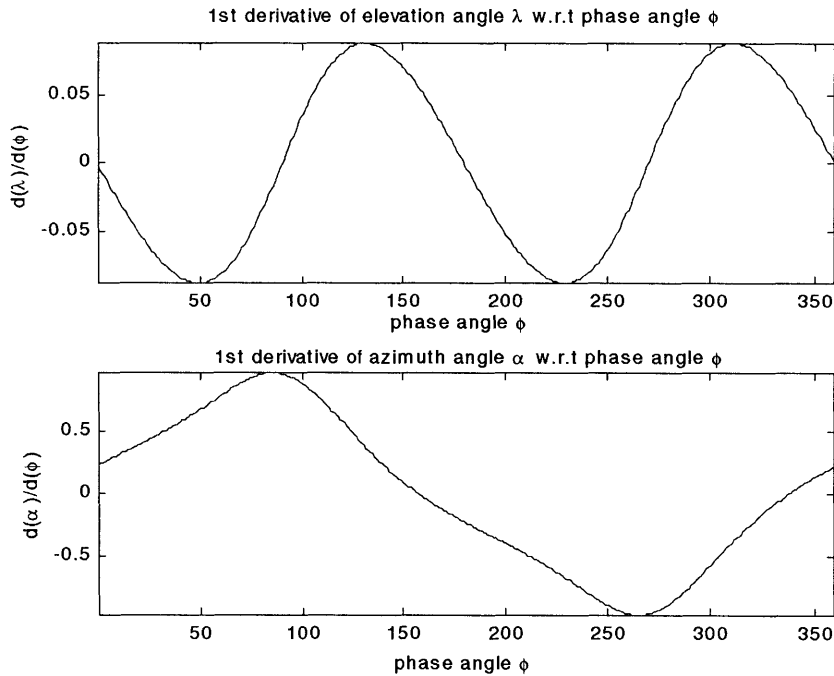
Figure 4-11: The 1st derivatives of the elevation and azimuth angles with respect to phase angle for the Walker configuration T/P/δ/F = 10/5/57.1°/2 and altitude = 1,550 km.

1st derivative of elevation angle λ w.r.t phase angle φ

1st derivative of azimuth angle α w.r.t phase angle φ
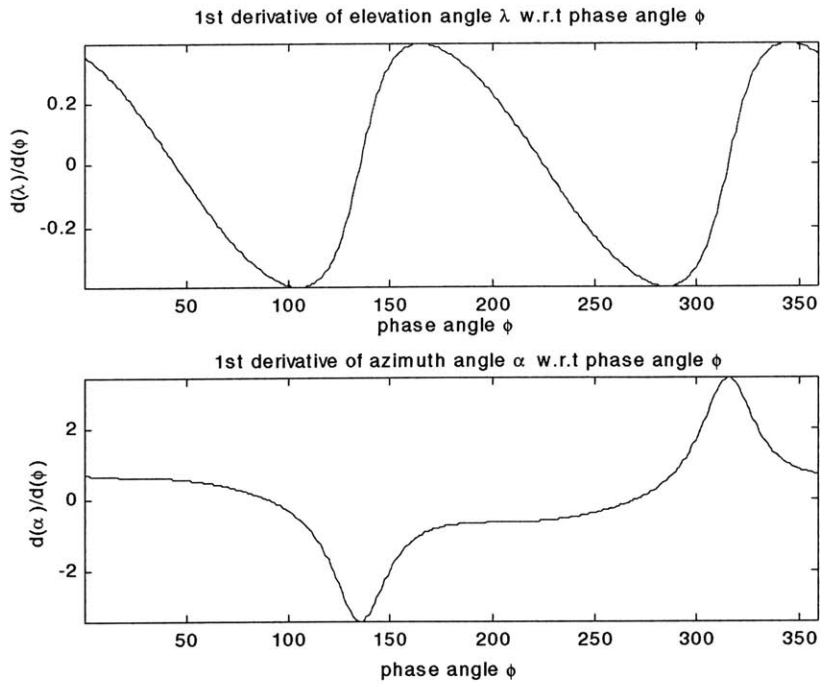
Figure 4-12: The 1st derivatives of the elevation and azimuth angles with respect to phase angle for the polar configuration P=2, S=3, and altitude = 15,000 km.

1st derivative of elevation angle λ w.r.t phase angle φ

1st derivative of azimuth angle α w.r.t phase angle φ

Figure 4-13: The 1ˢᵗ derivatives of the elevation and azimuth angles with respect to phase angle for the polar configuration P=2, S=4, and altitude = 15,000 km.

1st derivative of elevation angle λ w.r.t phase angle φ

1st derivative of azimuth angle α w.r.t phase angle φ

Figure 4-14: The 1ˢᵗ derivatives of the elevation and azimuth angles with respect to phase angle for the Walker configuration T/P/δ/F = 5/5/43.7 °/1 and altitude = 15,000 km.

38

Figure 4-15: The 1st derivatives of the elevation and azimuth angles with respect to phase angle for the Walker configuration T/P/δ/F = 4/2/45 °/1 and altitude = 15,000 km.

Constellation	Altitude(km)/T/P/δ/F	Max dλ/dϕ	Min dλ/dϕ	Max dα/dϕ	Min dα/dϕ
Polar LEO Space	1,550/12/2/90°/1.5	.3008	-.3008	1.5207	-1.5207
Polar LEO Earth	1,550/40/5/90°/2.5	.1811	-.1811	1.6693	-1.6693
Walker LEO	1,550/10/5/57.1°/2	.0711	-.0711	.5366	-.5366
Polar MEO Space	15,000/6/2/90°/1	.5230	-.5230	2.0066	-2.0066
Polar MEO Earth	15,000/8/2/90°/1	.5521	-.5521	2.6125	-2.6125
Walker MEO 1	15,000/5/5/43.7°/1	.0887	-.0887	.9641	-.9641
Walker MEO 2	15,000/4/2/45°/1	.3904	-.3904	3.4138	-3.4138

Table 4-2a: Summarization of the 1st-derivative intra-backbone link parameters w.r.t. ϕ for LEO and MEO constellations.

The above table lists the extreme values of dλ/dϕ and dα/dϕ. Now we must find the relationships between ϕ and time in order to derive the extreme values of dλ/dt and

dα/dt. To do this, we must first find the time it takes for the satellites of each altitude to complete a 360° orbit. We do this using the following equation for elliptical gravitational motion:

$$p^2 = \frac{4\pi^2 a^3}{GM} \qquad (4.13)$$

where p is the orbital period, a is the semi-major axis of the orbit (equal to the radius for our case), G is the gravitational constant, and M is the mass of the earth. For $G = 6.672\times10^{-8}$ cm^3/g/s^2 and M = 5.974×10^{27}g, the orbital periods work out to 7026s for the LEO orbit with an altitude of 1550km, 31,112s for the MEO orbit of 15,000km altitude, and 86,400s for a GEO orbit. Since each of these times represent a 360° progression of ϕ, we can relation ϕ to t and thus dϕ to dt for each of the orbits. Specifically, dϕ = .0512°/s•dt for the LEO orbit with h = 1,550 km, dϕ = .0116°/s•dt for the MEO orbit with h = 15,000 km, and dϕ = .0042°/s•dt for the GEO orbit with h = 35,786 km. Thus, a modified table 4-2, this time with dλ/dt and dα/dt instead of dλ/dϕ and dα/dϕ, can be calculated. It is included below.

Constellation	Altitude(km)/T/P/δ/F	Max dλ/dt	Min dλ/dt	Max dα/dt	Min dα/dt
Polar LEO Space	1,550/12/2/90°/1.5	.0154	-.0154	.0779	-.0779
Polar LEO Earth	1,550/40/5/90°/2.5	.0093	-.0093	.0855	-.0855
Walker LEO	1,550/10/5/57.1°/2	.0036	-.0036	.0275	-.0275
Polar MEO Space	15,000/6/2/90°/1	.0061	-.0061	.0233	-.0233
Polar MEO Earth	15,000/8/2/90°/1	.0064	-.0064	.0303	-.0303
Walker MEO 1	15,000/5/5/43.7°/1	.0010	-.0010	.0112	-.0112
Walker MEO 2	15,000/4/2/45°/1	.0045	-.0045	.0396	-.0396

Table 4-2b: Summarization of the 1st-derivative intra-backbone link parameters w.r.t. time for LEO and MEO constellations.

4.2 Intra-Plane Links

Different from the dynamic range and pointing angles of inter-plane links, the intra-plane cross-links of a satellite constellation have both a stationary range as well as stationary pointing angles. Figure 4-16 illustrates a typical intra-plane link, which occurs between the two black dots, representing backbone satellites.

Figure 4-16: A typical intra-backbone link, between S_1 and S_2.

Given this figure, we can quickly determine that the angle of elevation looking from S_1 to S_2 is $\frac{-360°}{2S}$, and the range from S_1 to S_2 is $2\bullet(R_e+h)\bullet\sin(360°/2/S)$. It can also be noted that the azimuth angle will be equal to $0°$, since the link is within a plane. We can now calculate the results for the intra-plane links of each constellation. The results are summarized in table 4-3.

Constellation	Altitude(km)/T/P/δ/F	Intraplane Range (km)	Intraplane λ (°)
Polar LEO Space	1,550/12/2/90°/1.5	11212	-45
Polar LEO Earth	1,550/40/5/90°/2.5	6068	-22.5
Walker LEO	1,550/10/5/57.1°/2	15856	-90
Polar MEO Space	15,000/6/2/90°/1	37028	-60
Polar MEO Earth	15,000/8/2/90°/1	30233	-45
Walker MEO 1	15,000/5/5/43.7°/1	N/A	N/A
Walker MEO 2	15,000/4/2/45°/1	42756	-90
GEO	35,786/3/1/0°/(N/A)	73030	-60
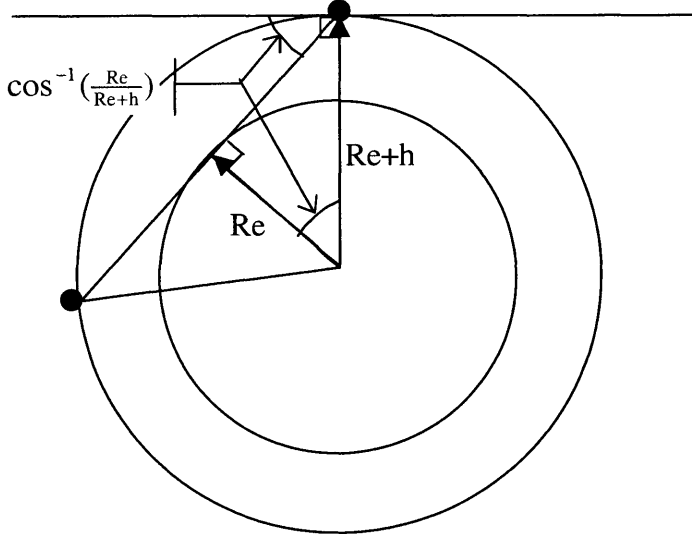
Table 4-3: Summarization of intra-plane backbone link for LEO, MEO and GEO constellations.

4.3 Constraint on Constellation Based on Backbone visibility

In order for the intra-plane backbone link to avoid obscuration by the earth, the angle of elevation of the intra-plane link has to be smaller than the angle of elevation from the satellite to the tangent point on the earth. Looking at figure 4-17, we see that this is the case when $\frac{360}{2S} < \cos^{-1}\left(\frac{Re}{Re+h}\right)$. Unfortunately, this means that intra-plane links are not possible for the Polar LEO Space, Walker LEO, and Walker MEO 2 configurations. In order for these intra-plane links to be possible, we must have the number of satellites per plane be at least
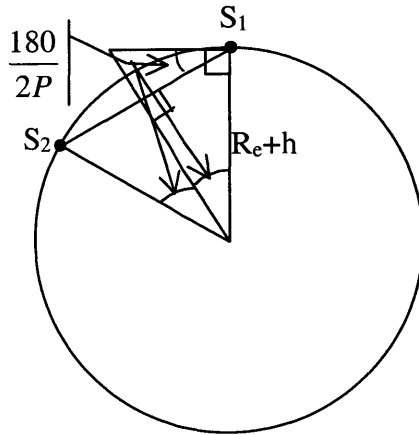
$$S = \left\lceil \frac{360}{2\cos^{-1}\left(\frac{Re}{Re+h}\right)} \right\rceil, \tag{4.14}$$

meaning that at the LEO altitude of 1,550 km, there must be at least 5 satellites per plane in order for the intra-plane link to be feasible. At the MEO altitude of 15,000 km, this means at least 3 satellites per plane are necessary.

42

Figure 4-17: The angle of elevation between a satellite and its tangent line to the earth.

Next, we apply this limit to the number of planes required in order for inter-plane links to be possible. We know that the maximum distance of an inter-plane link is at least the distance between planes at the equator. This angular distance is $180°/P$. The angle of elevation required to look from one satellite to another given this angular distance between the two is $180°/2/P$, as can be seen in figure 4-18.

Figure 4-18: An inter-plane link between S_1 and S_2. The circle drawn represents the equator of the sphere which contains the orbits of the satellites.

This angle, again, needs to be less than $\cos^{-1}\left(\frac{Re}{Re+h}\right)$, which is the angle of elevation between a satellite and its tangent to the earth. Thus, we have $\frac{180}{2P} < \cos^{-1}\left(\frac{Re}{Re+h}\right)$, making the minimum number of planes necessary to make inter-plane links possible at least

43
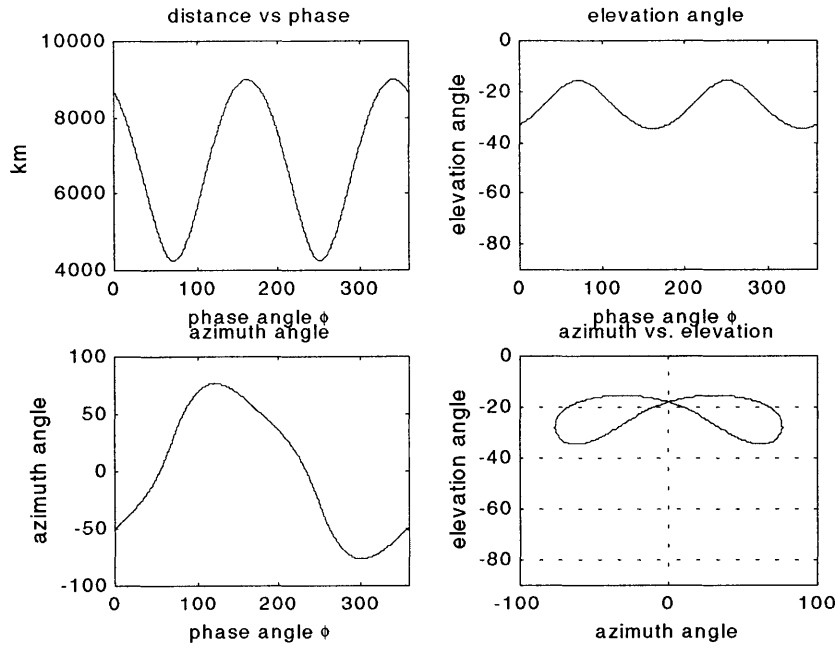
$$P = \left\lceil \frac{180}{2\cos^{-1}\left(\frac{Re}{Re+h}\right)} \right\rceil . \qquad (4.15)$$

For the LEO case, this evaluates to at least 3 planes, while for the MEO case, this evaluates to 2 planes.
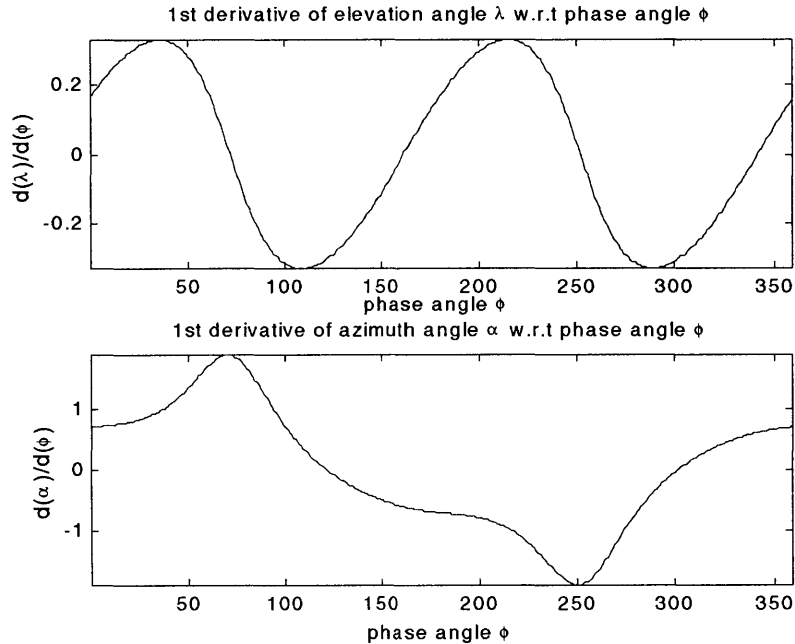
While the minimum MEO constellation is unchanged from before, we now see that the minimum LEO constellation required for backbone satellites to be visible to each other contains at least 5 satellites and at least 3 planes. This requirement essentially eliminates the satellite savings of the Walker LEO orbits, since they are now constrained to having at least 15 satellites, which is the same number as a polar constellation providing the same coverage and cross-link capabilities. Thus, the minimum LEO configuration should be polar, with 3 planes of 5 satellites each. We include the distance and pointing angle profile of this constellation below.

Constellation	Altitude(km)/ T/P/F	Max Range of Inter-plane link (km)	Max Azimuth Angle of Inter-plane link (°)	Min Elevation Angle of Inter-plane link (°)
Polar LEO Space	1,550/15/3/1.5	8,992	76.4	-34.5
Δ of Max and Min Elevation Angle Inter-plane link (°)	Max dλ/dt of Inter-plane link	Max dα/dt of Inter-plane link	Intra-plane link range (km)	Intra-plane link elevation (°)
-19.0	.0167	.0960	9320	-36

Table 4-4: Summary of 15-satellite polar constellation

Figure 4-19: Inter-plane cross-link parameter variations vs. phase angle for Polar configuration 15/5/90°/1.5, and altitude = 1550 km.

Figure 4-20: The 1st derivatives of the elevation and azimuth angles with respect to phase angle for the Polar configuration T/P/δ/F = 15/5/90 °/1.5 and altitude = 1550 km.

45

4.4 Final Constellations in Study

Ultimately, because we need to guarantee the availability of a space-to-ground link to any location on the globe, even possibly a mobile one, we need our constellations to cover the entire earth. Thus, we cannot utilize our minimal LEO and MEO constellations, but we must rather consider constellations which provide full ground coverage. Thus, from table 3-3, we must choose the 40-satellite constellation as our representative LEO and the 8-satellite constellation as our representative MEO. The GEO constellations can remain unchanged at 3 satellites. These three will be the constellations studied in the remainder of this thesis. The characteristics of these constellations are reprinted below from table 3-3.

	Altitude (km)	Total no of Sats (T)	No of Orbital Planes (P)	No of Sats per Plane (S)	Inclination of Planes (δ)	Phasing Parameter (F)
Polar LEO Earth	1,550	40	5	8	90°	2.5
Polar MEO Earth	15,000	8	2	4	90°	1
GEO	35,786	3	1	3	0°	N/A

Table 4-5: The final constellations under consideration in the study. All provide 100% coverage of all user orbits as well as full terrestrial coverage
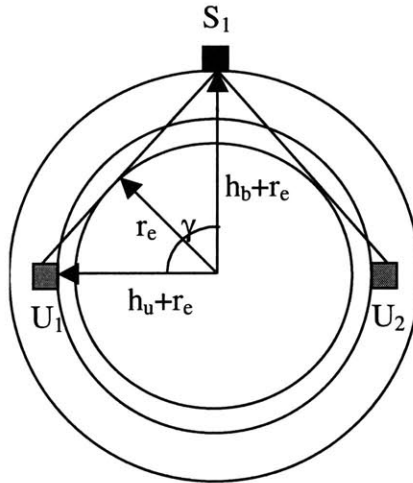
Chapter 5

Complexity of User-Access Links

For each of satellite constellations, we must assess the complexity of the user-access links. We do this by evaluating the following parameters: the maximum possible distance to a user and also the maximum possible slewing rate of an antenna servicing a user. We must also consider the number of apertures that must be carried by a backbone satellite in order to provide access to all users and any obscuration issues this may cause.

5.1 Upper-bound of Link Distance

The simplest estimate of upper-bound distance from a user satellite to a backbone satellite is the distance from the edge of the coverage region for each altitude class to the backbone satellite.

Figure 5-1: The coverage region of S_1

As illustrated by figure 5-1, this has the formula

$$d_{max} = \sqrt{(h_b + r_e)^2 - r_e^2} + \sqrt{(h_u + r_e)^2 - r_e^2} \qquad (5.1)$$

For LEO backbones at 1,550 km altitude, the maximum distance evaluates to 9333 km for LEO users at 1,500 km, 25113 km for MEO users at 15,000 km, and 46,388 for GEO

47

users. For MEO backbones at 15,000 km altitude, the result is 25,029km for LEO users, 40809 km for MEO users, and 62083 km for GEO users. For GEO backbones, the result is 46,303 km for LEO, 62,083 km for MEO, and 83,358 km for GEO. These results are summarized in table 5-1.

User Backbone	LEO (1500 km)	MEO (15,000 km)	GEO (35,786 km)
LEO (1550 km)	9333 km	25,113 km	46,388 km
MEO (15,000 km)	25,029 km	40,809 km	62,083 km
GEO (35,786 km)	46,303 km	62,083 km	83,358 km

Table 5-1: Summary of maximum distance from backbone to edge of coverage region

We do have an interest in reducing these maximum possible distance in cases where it is possible and convenient, however, since maximum link distance is a greater-than-linear factor in the cost of a cross-link, as we will later see. So, we will now look for ways of reducing the maximum possible user-access link distance where possible.

For the GEO backbone, this can be easily done, since the GEO coverage region is has radius >90° on user altitude classes. Thus, we can roughly divided each user altitude region into thirds centered around the nearest GEO backbone satellite, with a generous overlap of say 30° in order to accommodate make-before-break handoffs for LEO and MEO users. This scheme essentially assign to each GEO backbone satellite the users which are in the "half" of the user sphere closest to it, i.e. the users which are close to the backbone satellite than to its antipodal position. The furthest LEO and MEO users, then, would be on the edge of a coverage region of radius 90°, meaning their distance from the backbone satellite would be the hypotenuse of a triangle with sides $r_e + h_{GEO}$ and $r_e + h_{MEO/LEO}$. The furthest such users for MEO is then $\sqrt{(6,378+35,786)^2 +(6,378+15,000)^2} = 47,273\,\text{km}$ away, and the furthest LEO users is $\sqrt{(6,378+35,786)^2 +(6,378+1,550)^2} = 42,902\,\text{km}$ away. For GEO users, we would not need the overlap for hand-offs, since the backbone satellite and the user remain stationary to each other. Thus, we simply break up the GEO user plane into thirds centered around each backbone satellite. This means that the furthest users will be at most 60° away from the

GEO backbone in central angle. If a user is 60° away on the GEO plane, the backbone satellite, user satellite, and the center of the earth make an equilateral triangle, making the maximum service distance $r_e + h_{GEO} = 6,378 + 35,786 = 42,164$ km.

For the MEO and LEO backbone constellation, we will discover in the next sections that in the interest of reducing aperture count, we utilize nearly the entire coverage region of a backbone satellite, especially on the GEO user plane. Thus, the distance from a backbone satellite to the edge of a coverage region remains a good estimate for the maximum user-access link distance for MEO and LEO backbones. We will summarize the revised estimates for maximum user-access link distance in the table below.

Backbone \ User	LEO (1500 km)	MEO (15,000 km)	GEO (35,786 km)
LEO (1550 km)	9333 km	25,113 km	46,388 km
MEO (15,000 km)	25,029 km	40,809 km	62,083 km
GEO (35,786 km)	42,902 km	47,273 km	42,164 km

Table 5-2: Summary of estimated maximum distance of user-access link
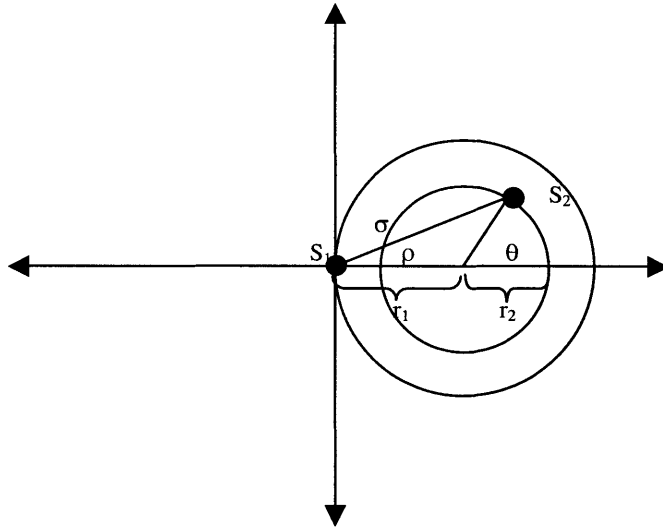
5.2 Upper-bound of Slewing Rate

We now wish to find the upper bound on the possible slewing rates of the user link. For given backbone and user altitudes, we now argue that the maximum slewing rate occurs when the user satellite and backbone satellite are right above and below one another, meaning they are collinear with the earth's center. This is because this situation minimizes the distance between the satellites, while the magnitude of the velocity vectors of the satellites only depend on their altitudes and therefore are constant over all satellite locations at given altitudes. We know that the rate of angle variation between the two satellites is inversely related to the distance between them. Thus, if the magnitudes of the velocity vectors are the same and we've minimized the distance between them, then we have maximized the slewing rate between them. Thus, we achieve maximum slewing rates when the two satellites are right above and below one another.

With this constraint, we can still rotate the velocity vectors with respect to each other in order to find the maximum slewing rate for a single direction. This direction

49

occurs when the velocity vectors are at 180° from each other, since in this direction the magnitudes of the vectors contribute only to one direction. The physical situation that this represents is two satellites orbiting in retrograde directions in the same orbital plane.

We now want to find an expression for the variation of the angle formed by the link between two retrograde-orbiting satellites and the plane tangent to the orbit of the backbone satellite over one period.

Figure 5-2: Calculating the maximum slewing rate in a retrograde satellite configuration.

Looking at figure 5-2, consider the link between S_1 and S_2, with S_1, the backbone satellite, orbiting clockwise and S_2, the user, orbiting counter-clockwise. If we were to stay in a frame where S_1 remained stationary at the origin, we could consider S_2 as rotating twice as fast around the center of the concentric circles. Consider the angle that the link makes with the y-axis when S_2 has gone through a rotation of θ degrees. We know that S_2 has the coordinates $(r_2\cos(\theta)+r_1, r_2\sin(\theta))$. Thus, the angle ρ between the link and the x-axis is

$\tan^{-1}\left(\dfrac{r_2\sin(\theta)}{r_2\cos(\theta)+r_1}\right)$, and the angle σ, which represents the angle of "elevation" between

the tangent of the backbone satellite and the link to the user satellite, is 90°-ρ.

Differentiating ρ with respect to θ, we obtain the expression $\dfrac{d\rho}{d\theta} = \dfrac{r_2^{\,2} + r_1 r_2 \cos\theta}{r_1^{\,2} + r_2^{\,2} + 2r_1 r_2 \cos\theta}$.

We know that $\theta = 2\phi$, where ϕ is the actual phase angle of the orbit, since we made an

adjustment in the frame of reference. Thus, we know that the slewing rate with respect to phase angle is

$$\frac{d\rho}{d\phi} = 2\frac{d\rho}{d\theta} = \frac{2r_2{}^2 + 2r_1 r_2 \cos\theta}{r_1{}^2 + r_2{}^2 + 2r_1 r_2 \cos\theta} \qquad (5.2)$$

Differentiating and setting this expression equal to zero, we can see that it has extremal values at $\theta = \pi$, which would make the maximum value of $d\rho/d\theta$ equal to

$$\frac{2r_2{}^2 - 2r_1 r_2}{r_1{}^2 + r_2{}^2 - 2r_1 r_2} . \qquad (5.3)$$

Now we must find the relationships between ϕ and time in order to derive the extreme values $d\rho/dt$. To do this, we must first find the time it takes for the satellites of each altitude to complete a 360° orbit. We do this using the following equation for elliptical gravitational motion:

$$p^2 = \frac{4\pi^2 (r_1 + r_e)^3}{GM} \qquad (5.4)$$
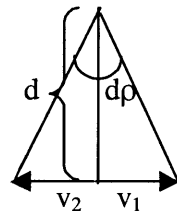
where p is the orbital period, $(r_1 + r_e)$ is the semi-major axis of the orbit (equal to the radius for our case), G is the gravitational constant, and M is the mass of the earth. For G = 6.672×10⁻⁸ cm³/g/s² and M = 5.974×10²⁷g, the orbital periods work out to 7026s for the LEO orbit with an altitude of 1550km, 31,112s for the MEO orbit of 15,000km altitude, and 86,400s for a GEO orbit. Since each of these times represent a 360° progression of ϕ, we can relate ϕ to t and thus $d\phi$ to dt for each of the orbits. Specifically, $d\phi$ = .0512°/s•dt for the LEO orbit with h = 1,550 km, $d\phi$ = .0116°/s•dt for the MEO orbit with h = 15,000 km, and $d\phi$ = .0042°/s•dt for the GEO orbit with h = 35,786 km. Thus, the expression for the maximum slewing rate is

$$\frac{d\rho}{dt}\bigg|_{max} = \frac{2r_2{}^2 - 2r_1 r_2}{r_1{}^2 + r_2{}^2 - 2r_1 r_2} * \frac{360}{\sqrt{\dfrac{4\pi^2 (r_1 + r_e)^3}{GM}}} \qquad (5.5)$$

For the LEO case where r_1 =1,550 + r_e and r_2 = 1,500 + r_e, this expression evaluates to
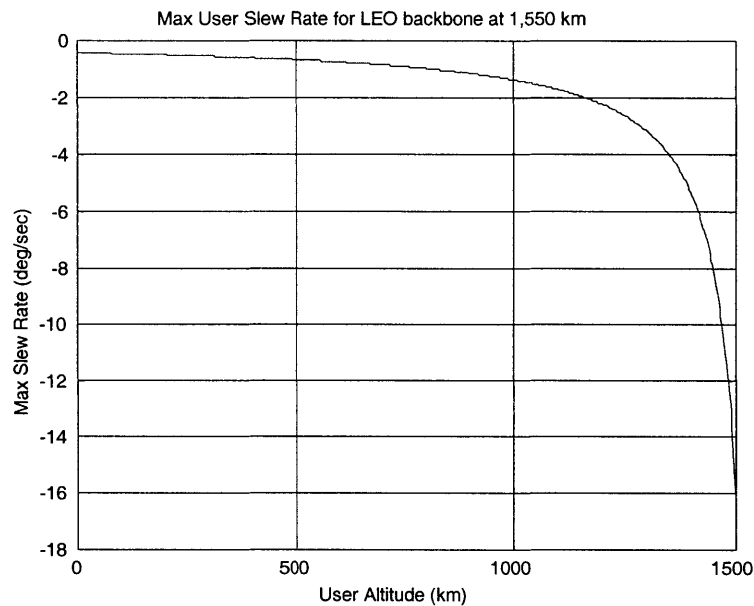
-16.13 °/s. As a sanity check, this is consistent with the result obtained by the method illustrated in figure 29, which involves adding the two opposing instantaneous satellite

51

velocity vectors and then evaluating the angle of change at a distance d km away. The expression obtained using this method is $\frac{d\rho}{dt} = 2\tan^{-1}\left(\frac{v_1 + v_2}{2d}\right)$, which evaluates to $-$ 16.17°/s.
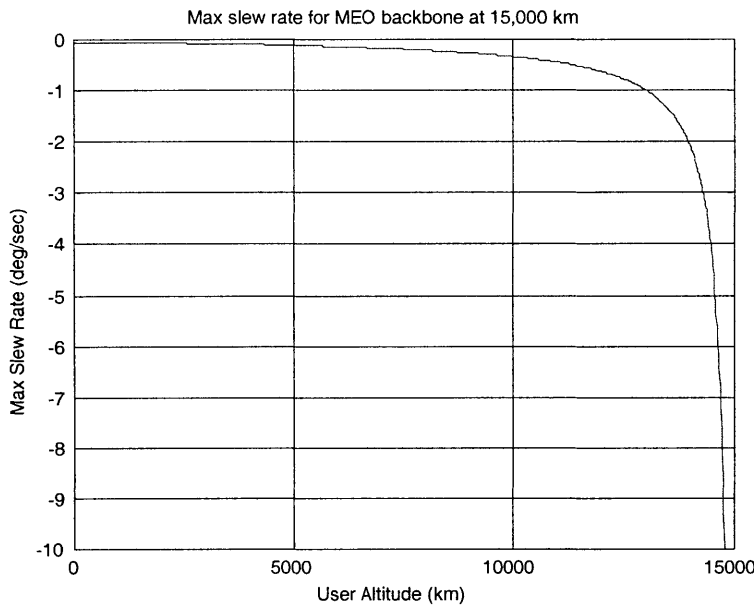
Figure 5-3: A sanity check on slew rate calculations

We have plotted the max slew rate versus user altitude for the LEO and MEO backbone cases below.
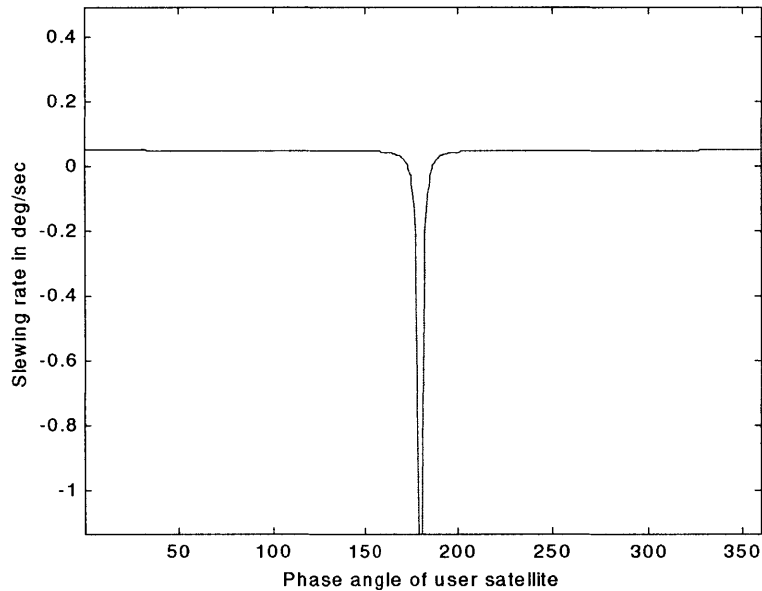
Figure 5-4: Maximum slew rate of user-link for a LEO at 1,550 km altitude

Max slew rate for MEO backbone at 15,000 km
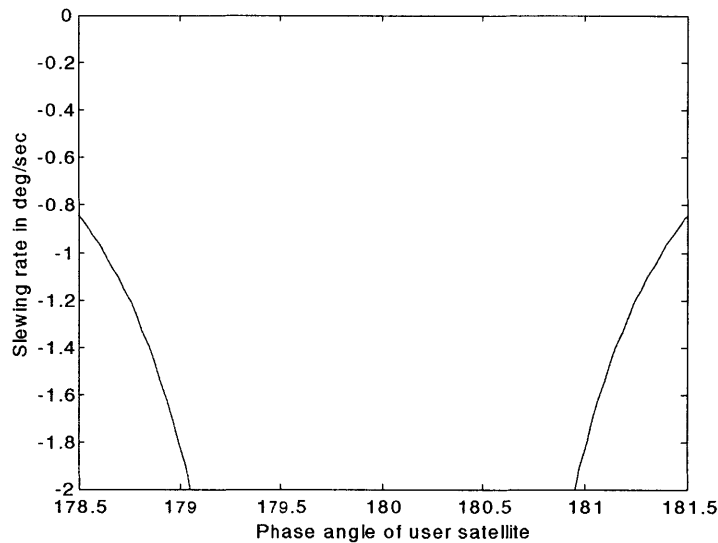
Figure 5-5: Maximum slew rate of user-link for MEO backbone at 15,000 km

At backbone altitude 1,550 km and user altitude 1,500 km, the plot of the slew rate versus θ is as follows:
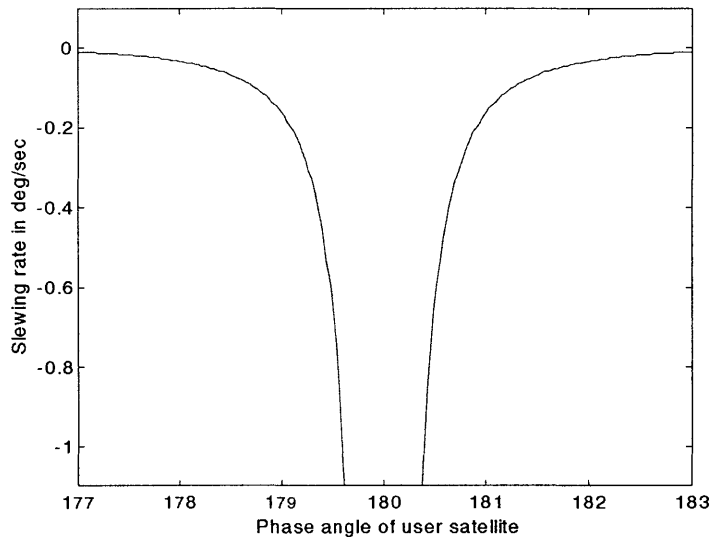
Figure 5-6: Slewing rate vs. Phase angle of user satellite of 1,500km altitude with LEO backbone at 1,550 km altitude.

as we can see, the slewing rate is a constant less than .1 °/s for a majority of the orbit and only increase to a maximum around -16°/s for a small band around θ = 180° which exceeds –1°/s only for a band of less than 3 degrees from θ = 178.5° to 181.5°, as shown in figure 5-7, a zoomed in version of figure 5-6.

Figure 5-7: A close-up of figure 5-6.

In the MEO case with a separation of 50 km between the two satellites, the region of the user orbit where the slewing rate exceeds -1°/s is even narrower, ranging only from θ = 179.5° to 180.5°, as can be seen in the next figure.

Figure 5-8: Slewing rate vs. Phase angle of user satellite with MEO backbone at 1550 km altitude.

For user altitude equal to backbone altitude, we have a situation where ρ is always increasing at ½ the rate as θ, by a geometric theorem. Thus, except for the instantaneous change in direction at θ = 180°, the slewing rate remains constant and is equal to dφ/dt, or the rate of change in phase angle with respect to time. This is .0512 °/s for the LEO case and .0116°/s for the MEO case.

Based on the very small proportion of user orbits around the backbone satellite where the slewing rate exceeds the feasible range, we can conclude that service outage due to tracking difficulty caused by excessive slewing rate can be easily overcome by hand-off to a neighboring backbone satellite. And since these excessive slewing rates only occur when a user satellite is near one backbone satellite, we can guarantee its visibility by another backbone satellite, because backbone satellites were designed visible to at least their neighbors in the same orbital plane in order to maintain intra-backbone links. Thus, we can conclude that maximum slow rates do not pose a limiting consideration in the choice of our constellation.

55

5.3 Number of Apertures Required for User Support

Given the nature of high-rate space communication, antenna apertures must be devoted to user connection on a one-to-one basis. Theoretically, the minimum number of apertures that must be carried by the backbone constellation is equal to the expected number of users. Additionally, it would be desirable for manufacturing reasons to place an equal number these apertures on all the satellites forming the backbone. Thus, the most ideal situation would be if each backbone satellite carried $\left\lceil \dfrac{u}{n} \right\rceil$ apertures, where u is the total number of users and n is the total number of backbone satellites.

In practice, however, more apertures will be placed on each backbone satellite than the ideal theoretical minimum for several reasons. First, the geometry of backbone satellite coverage affects how many apertures each individual satellite must carry. In the first subsection, we will examine how the geometry of overlapping coverage regions dictate the number of apertures carried by an individual satellite and determine an expression for the number of apertures that a satellite must carry as a function of its coverage characteristics. Next, we will look at the backbone-user combinations case-by-case, beginning with the GEO backbone-GEO user situation, to see how many apertures are necessary to provide service for each combination. To simplify analysis for this section, we will assume that users of all orbital classes are uniformly distributed within their space.

The second cause for an increased number of apertures onboard a backbone satellite is the necessity of user hand-offs between backbone satellites. More than one aperture must be devoted to a single connection in order to ensure a safe make-before-break hand-off. Thus, at all times we wish to have some number of apertures free on each backbone satellite in order to service these hand-offs, creating the need for satellites to carry extra apertures over the number determined by geometry. We will examine the hand-off requirements for each backbone constellation to see how they necessitate additional apertures on each backbone satellite. As a conclusion, we will provide a recommendation for the number of apertures that must be placed aboard the individual

56
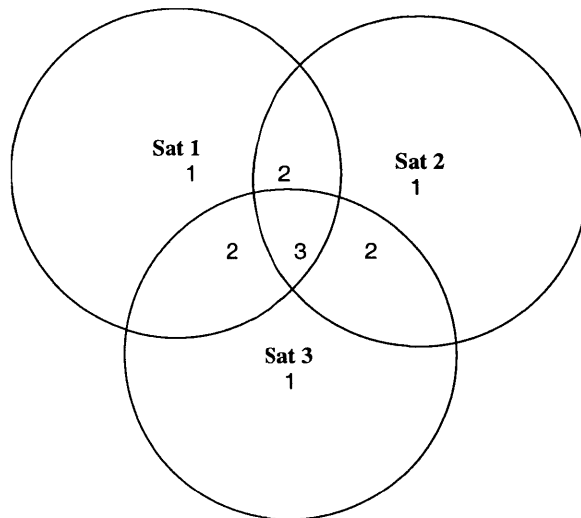
satellites of each backbone constellation and also suggest physical locations onboard the satellites for their placement.

5.3.1 Effects of Geometry on Number of Apertures

Consider the coverage region of a single backbone satellite at a snapshot in time, say sat 1 in figure 5-9. This particular backbone satellite is responsible for providing service to all of the user satellites in its coverage region unless its region overlaps the region of another backbone satellite, like the intersection between sat 1 and sat 2 in figure 5-9, in which case the users in the overlapping region can be divided among the two backbone satellites. If there more than two overlapping regions (like the center region of figure 5-9), then the users can be divided among all of the satellites with overlapping coverage regions. Thus, a backbone satellites must provide one aperture for every satellite in its single coverage region, one aperture for every two satellites in a coverage region it shares with another backbone satellite, and so on. We capture this in the equation

$$a_j = \sum_{c_j} \left\lceil \frac{u_i}{i} \right\rceil \tag{5.6}$$

where a_j is the number of apertures that backbone satellite j must carry, c_j is j's coverage region, i is the level of coverage that the user experiences, and u_i is the number which experience i-levels of coverage.

Figure 5-9: The overlapping coverage regions of three backbone satellites.

Now given the uniform distribution of users assumption, we can modify the previous equation as follows

$$a_j = \left\lceil \frac{u}{v} \left(\int_{c_j} \frac{1}{i} dV \right) \right\rceil \qquad (5.7)$$
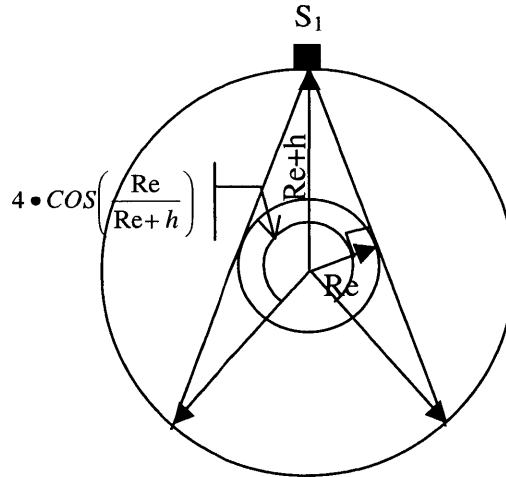
where a_j is the number of apertures that backbone satellite j must carry, c_j is j's coverage region, i is the level of coverage experienced by dV, u is the total number of users, and v is the total volume of the space of possible user locations. We will assume that a_j will be the same for all backbone satellites, since orbital regularities will cause each satellite to experience the same maximum level of user demand given the uniform user assumption. In the most desirable case, we want this number to be $\left\lceil \frac{u}{n} \right\rceil$, where n is the number of backbone satellites, for all satellites, which will waste the least number of apertures while providing access for all users. We will now examine the backbone-user combinations case-by-case to see if they will yield this desirable result.

5.3.2 GEO Backbone

5.3.2.1 GEO backbone-GEO User

When a GEO backbone is serving GEO users, each GEO covers $4 \bullet \cos\left(\dfrac{Re}{Re+h}\right)$

= 325.2° of the GEO orbit, out of a total of 360°, as figure 5-10 illustrates. The coverage gap of one single satellite is thus 360°-325.2° = 34.8°.
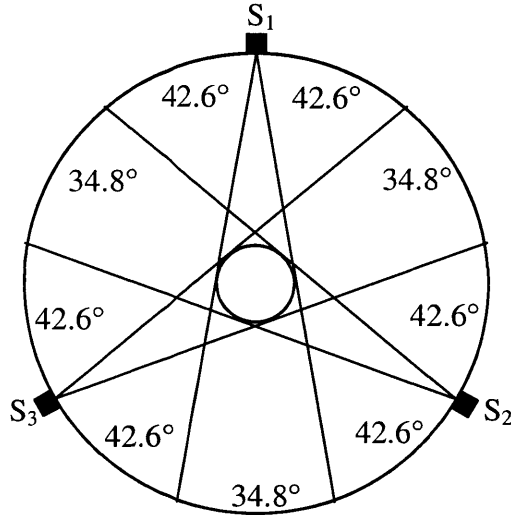
Figure 5-10: GEO backbone coverage of GEO users.

For $n \geq 2$ evenly spaced backbone satellites and assuming a uniform distribution of users, we theorize that the user load can be evenly split among the backbone satellites, because the obscured region of each individual backbone satellite is small, thus facilitating an easy division of users. For the common three-satellite GEO backbone, we see that this is indeed that case. Referring to figure 5-11, we see that the coverage region of a single backbone satellite includes 2*34.8° of double coverage and 6*42.6° of triple coverage. Substituting this into equation 5.7, we get

$$a_j = \left\lceil \frac{u\left(\dfrac{2}{2} \bullet 34.8° + \dfrac{6}{3} \bullet 42.6°\right)}{360°} \right\rceil \tag{5.8}$$

$$a_j = \left\lceil \frac{u}{3} \right\rceil$$

59

Thus, for u_g GEO user satellites and 3 backbone satellites, the total number of apertures

that each GEO backbone has to carry in order to service GEO users is $\left\lceil \dfrac{u_g}{3} \right\rceil$.
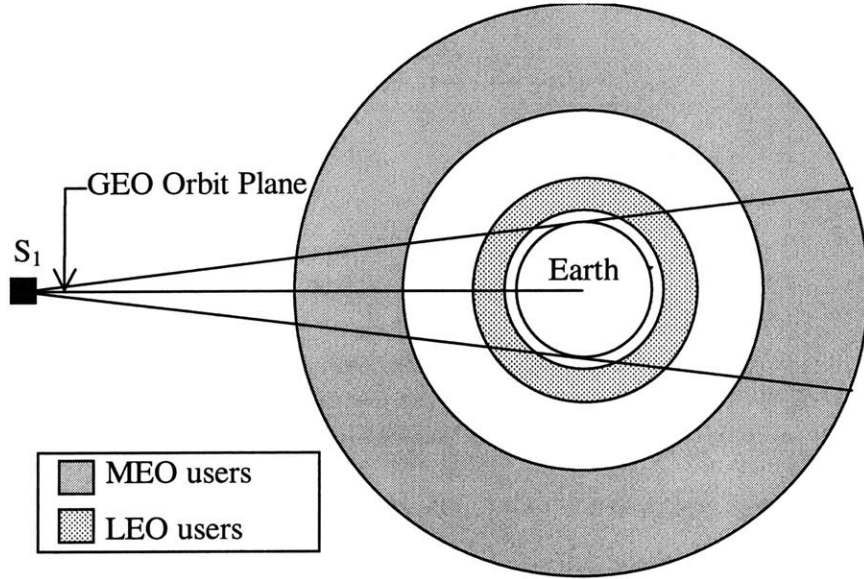
Figure 5-11: Illustration of the coverage regions of a 3-satellite GEO backbone
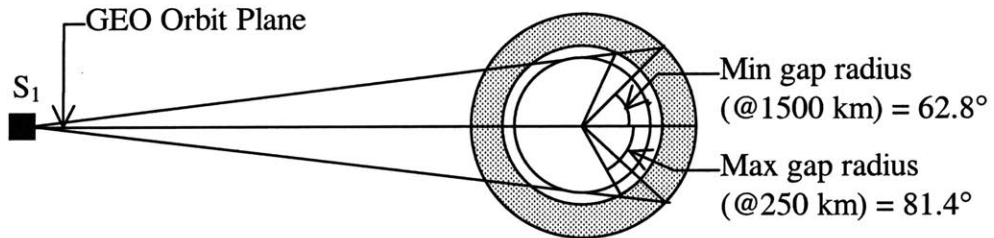
5.3.2.2 GEO backbone-MEO/LEO User

A GEO backbone satellite services MEO/LEO users from a "higher" altitude, that is, from an orbit of greater radius than the user. As figure 5-12 suggests and equation 3.1 confirms, if we consider spheres of successively increasing radii in the LEO/MEO user altitude ranges, the percentage of the sphere that can be covered by a single GEO satellite monotonically increases with the radii. If coverage can be evenly divided amongst the backbone satellites on all spheres of infinitesimal "thickness" and increasing radii within the LEO and MEO altitudes, then we can naturally conclude that all LEO and MEO users can be divided evenly amongst the backbone satellites, since we may simply "integrate" the regions assigned to individual backbone satellite over all altitudes to produce an even division of the total LEO/MEO user space. We need only to show that coverage of the sphere at the lowest LEO altitude can be evenly distributed amongst GEO backbone satellites in order to demonstrate the existence of an even distribution of coverage for the whole LEO/MEO user space. This is due to the fact that coverage regions of individual backbone satellites monotonically increase in size with increasing user altitude around the

same sub-satellite point. Thus, a valid distribution scheme of a low user altitude remains valid at a higher user altitude, since the coverage region of a backbone satellite on a user sphere of higher altitude is a superset of the coverage region of the same backbone on a user sphere of a lower altitude. Thus, we will now demonstrate the existence of evenly distributed coverage for a three-GEO constellation on a user sphere of 250km altitude and conclude the existence of evenly distributed coverage for the three-GEO constellation for all LEO and MEO users.

Figure 5-12: A GEO backbone satellite providing service to the MEO and LEO user regions.
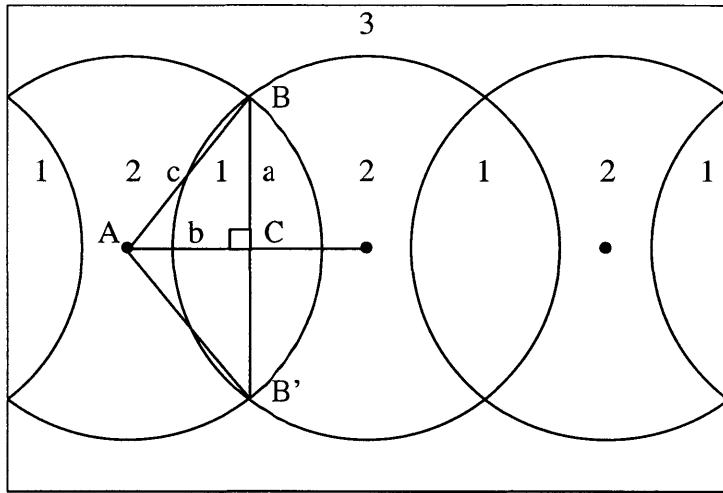
Figure 5-13: The coverage gap for a GEO backbone and the LEO user region.

For a given user altitude, we recall that we can calculate the radius of coverage by a single GEO satellite on the sphere at that altitude via the equation

$$\gamma = \cos^{-1}\left(\frac{r_e}{R_1}\right) + \cos^{-1}\left(\frac{r_e}{R_2}\right) \tag{3.1}$$

where γ is the radius in angular distance, r_e is the radius of the earth, R_1 is the radius of the backbone and R_2 is the radius of the user sphere. For a GEO backbone and LEO users,

this coverage radius is smallest at the lowest user altitude of 250 km, with a value of 97.1°, making the radius of the coverage gap 82.9°. When the 250 km altitude user sphere is projected onto a plane, this coverage profile will appear like figure 5-14, with regions of single, double, and triple coverage.

Figure 5-14: The projection of a GEO backbone's coverage region on the 250 km altitude LEO user sphere. The circles indicate the coverage gaps of individual backbone satellites, thus the numbers within the regions indicate the level of coverage of that particular region.

We will now use several equations from spherical geometry to calculate the surface areas of the various regions, to determine if the GEO backbone can provide maximally efficient service on this sphere. First, we calculate the area of each individual circle, which is given by the formula

$$A_c = 2\pi R^2(1\text{-cos } r) \tag{5.9}$$

Where R is the radius of the sphere and r is the radius of circle in central angle degrees. For the GEO backbone and 250 km LEO user case, this area becomes $2\pi R^2(1\text{-cos } 81.9°)$ = $5.51R^2$. Next, we must calculate the areas of the "overlap" regions between the circles, which are the areas of single coverage with the help of three more formulas from spherical geometry. The first is the law of sines for spherical triangles, which is

$$\frac{\sin A}{\sin a} = \frac{\sin B}{\sin b} = \frac{\sin C}{\sin c} \tag{5.10}$$

where A, B, and C are the angles of the spherical triangle, which are the angles formed by tangents to the arcs representing the sides at their particular intersection, and a, b, and c

are the lengths of the sides of the spherical triangle measured in degrees of central angle. The second is a formula for spherical right triangles, which says, for a spherical triangle with a right angle at C,

$$\cos A = \sin B \cos a \ . \tag{5.11}$$

And the third is Girard's formula, which says that the surface area of a spherical triangle with angles A, B, and C measured in radians is

$$A_t = R^2(A+B+C-\pi) \tag{5.12}$$

In order to find the area of the single coverage region, we will find the area of the "pie" shaped region formed by A, B and B', subtract out the area of the triangle ABB', and finally double this difference.

We first notice that $\angle C = 90°$ because all of the subsatellite points are equatorial and the coverage regions have equal radius. Next, we can label side b = 60°, half of the distance between subsatellite points, and side c = 82.9°, the radius of the coverage hole. We can then find $\angle B$ by the spherical sine formula

$$\angle B = \sin^{-1}\left(\frac{\sin 90° \sin 60°}{\sin 82.9°}\right) = 60.77° \ . \tag{5.13}$$

With this, we can find $\angle A$ by equation (5.11),

$$\angle A = \sin^{-1}\left(\frac{\cos 60.77°}{\cos 60°}\right) = 77.59° \tag{5.14}$$

So, the area of the spherical right triangle ABC is

$$A_{ABC} = \pi R^2\left(\frac{77.6° + 60.8° + 90° - 180°}{180°}\right) = .844R^2, \tag{5.15}$$

meaning that the area of ABB' is $1.688R^2$. The area of the pie-shaped region is

$$A_{Pie} = \frac{2*77.69}{360} * 5.51R^2 = 2.375R^2. \tag{5.16}$$

So the area of one single coverage region is

$$A_{Single} = 2(2.375R^2 - 1.688R^2) = 1.374R^2 \tag{5.17}$$

The area of each individual double coverage region is

$$A_{Double} = 5.51R^2 - 2*1.374R^2 = 2.762R^2, \tag{5.18}$$

and the area of the triple coverage region is

$$A_{Triple} = 4\pi R^2 - 3(A_{Single}) - 3(A_{Double}) = .157R^2. \tag{5.19}$$

Each individual satellite can see one single coverage region, two double coverage regions, and all of the triple coverage region. Therefore, it is responsible for the following fraction of users

$$F_{GEO-LEO} = \frac{1.374 + \frac{2(2.762)}{2} + \frac{.157}{3}}{4\pi} = .333, \tag{5.20}$$

which demonstrates that a three-satellite GEO backbone is capable of providing maximally efficient coverage in terms of apertures to the 250 km LEO user sphere and thus to all LEO and MEO users.

5.3.2.3 Hand-offs

The previous section took into account the distribution of apertures on the three-satellite GEO backbone given uniformly distributed stationary users. We know, however, that users do not remain stationary but travel in their orbit. Thus, we must take into account the need for make-before-break hand-offs as users travel from the coverage regions of one backbone satellite to another. Ideally, we can devote just one single aperture to this task above and beyond the number required to provide normal service to the users. To examine the feasibility of achieving this ideal situation, we will now estimate the rate of hand-offs required to see if a single free aperture can keep up. We need only to consider LEO users in this discussion. This is because GEO users are stationary with respect to backbone satellites, and the large (radius ~90°) overlapping coverage regions and long user orbital periods at MEO altitudes provide periods of hours in which a hand-off can be performed, making scheduling a simple task. Thus, we will only consider the LEO users..

A hand-off is only truly necessary when a satellite travels from one single-coverage region to another single-coverage region. Thus, in our calculations, we will adapt the estimate that half of the user within a single-coverage region will travel toward the eastwardly neighboring single-coverage region and half will travel toward the westwardly neighboring single-coverage region. We also consider all of these satellites to be at a

uniform altitude and the path they must travel between single-coverage regions to all have the shortest distance, which is the distance along the equatorial orbit. Referring to figure 39, this distance is twice the difference of the distance between sub-satellite points and the radius of the coverage hole, which for the 250km orbit is $2*(120°-82.9°)=74.2°$. Estimating the orbital period to be 90 minutes, this leaves $74.2/360*90=18.5$ minutes perform all of the hand-offs. The single coverage region has a surface area of $1.374R^2$, which is $1.374/(4\pi) = .11$ of the total surface area of the sphere. Thus, we can expect a maximum .11 of the total number of LEO users to require hand-off to a particular satellite at a time. With 30-40 LEO users expected in total, this means that at most 4-5 satellites will require transition to a particular backbone satellite at a time. With 18.5 minute as the shortest amount of orbit time between single coverage regions, this allows an average of at least 3 minutes per hand-off, which should be a rate that can be maintained even considering antenna slewing time and also time required to negotiate a new connection. Thus, for a 3 satellite GEO backbone, one additional aperture per satellite seems sufficient to meet the necessary hand-off requirements.

5.3.3 MEO Backbone

5.3.3.1 MEO Backbone-GEO User
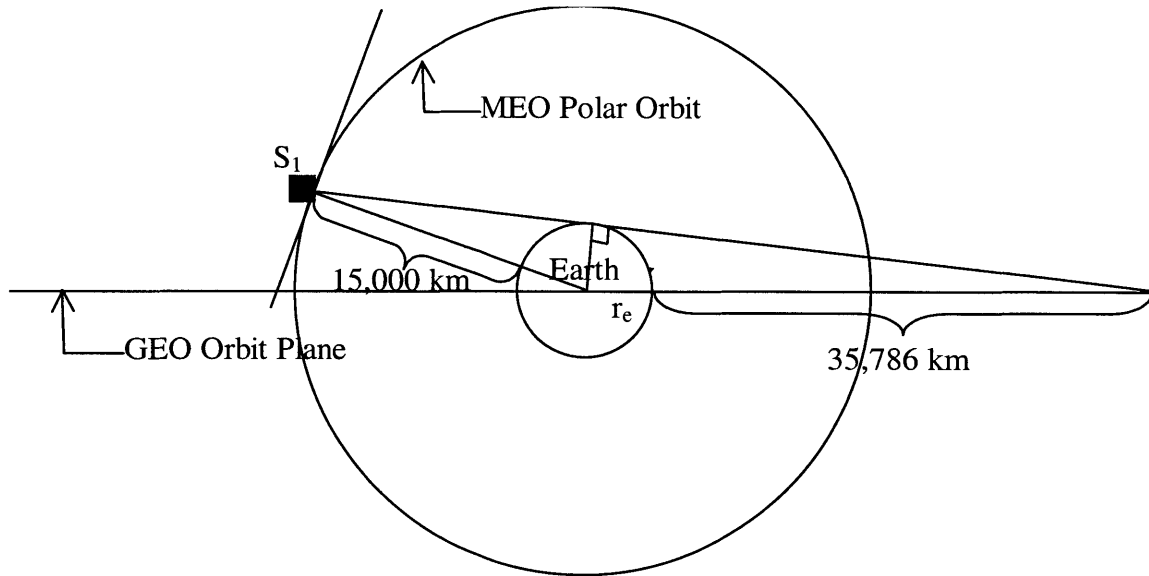
To begin our analysis of the MEO backbone, we must first consider if it can effectively provide coverage for GEO users. This analysis differs from that of a GEO backbone serving GEO users because the MEO backbone satellites orbit in planes perpendicular to the GEO user plane, whereas GEO backbone satellites remain co-planar with GEO user satellites. Thus, the amount of coverage that a constellation of MEO satellites can provide to the GEO user plane varies dynamically over time. In our analysis of MEO backbone with GEO users, then, we will develop a simplified dynamic model of the visibility of the GEO user plane to the MEO backbone satellites and use this simplified model to determine the efficiency of MEO backbone coverage for GEO users.

The profile of the coverage region of a single MEO satellite is shown in figure 5-15 below. As one can visualize, while the MEO backbone satellite S_1 is above the equator, its view of the opposite side of the GEO orbit plane is obscured by the earth.

This obscuration begins to lessen as S_1 orbits toward the polar regions until all of the GEO orbital plane is visible when S_1 nears the polar regions. From figure 40, the place at which this total visibility occurs is at

$$180^\circ - \cos^{-1}\left(\frac{r_e}{r_e + 35,786}\right) - \cos^{-1}\left(\frac{r_e}{r_e + 15,000}\right) = 26.1^\circ \qquad (5.21)$$

past the equator.
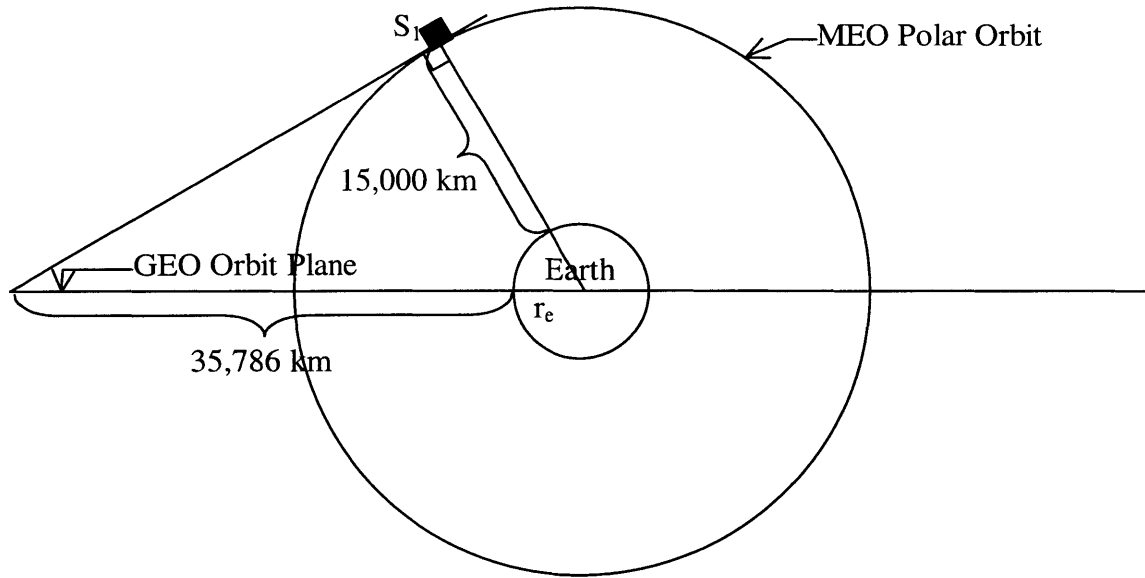
Figure 5-15: The visibility of the GEO orbit plane from a MEO polar orbit.

By examining the tangent line at that location, however, we realize that in order to utilize this "visibility" by providing service to the entire GEO, a MEO satellite at this altitude would have to mount apertures on both its "earth-facing" surface and the surface opposite that one, which we call the "space-facing" surface. We would like to avoid apertures on the space-facing surface, since they do not point toward any possible users when the backbone satellite is near the poles. On the other hand, apertures mounted on the earth-facing surface always point toward possible users of various altitudes. Thus, we would like to find the point where the whole GEO plane is visible from the earth-facing surface. This occurs when the tangent to the MEO polar orbit intersects the GEO orbit ring, which is illustrated in figure 5-16. S_1 is at

$$\cos^{-1}\left(\frac{re + 15,000}{re + 35,786}\right) = 59.5^\circ \qquad (5.22)$$

66
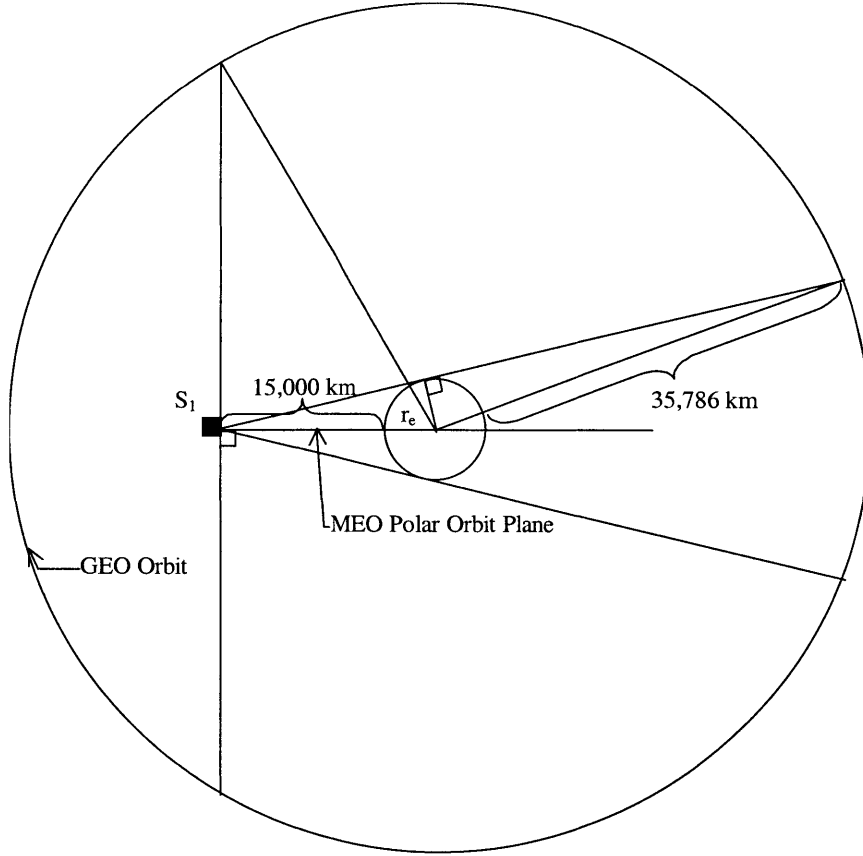
past the equatorial plane when this occurs. Thus, we can say that for 60° portions centered around the poles, the MEO backbone satellite can service all of the GEO plane.

Now, for the rest of the orbit, we make the simplifying assumption that the obscuration due to the earth is the same as it is when the backbone satellite is at the equator. Since the earth's circumference is greatest in the equatorial plane, we can assume that the obscuration of visibility from the polar MEO satellite orbit to the equatorial GEO orbit is greatest over the equator. Our assumption is then a worst-case simplification, whereby if there is any obscuration, we assume it to be have the greatest effect possible.

Figure 5-16: Full visibility of the GEO plane from a polar MEO using only the earth-facing surface.

When the MEO backbone satellite is over the equator, its visibility of the GEO orbit is shown in figure 5-17. The equation for the "hole" in visibility is

Figure 5-17: The visibility of the GEO plane from a MEO satellite 15,000 km over the equator.

$$2*(180° - \cos^{-1}\left(\frac{r_e}{r_e + 35{,}786}\right) - \cos^{-1}\left(\frac{r_e}{r_e + 15{,}000}\right)) = 52.2° \qquad (5.23)$$

Thus the MEO backbone satellite above the equator is visible to 308° of the GEO orbit.
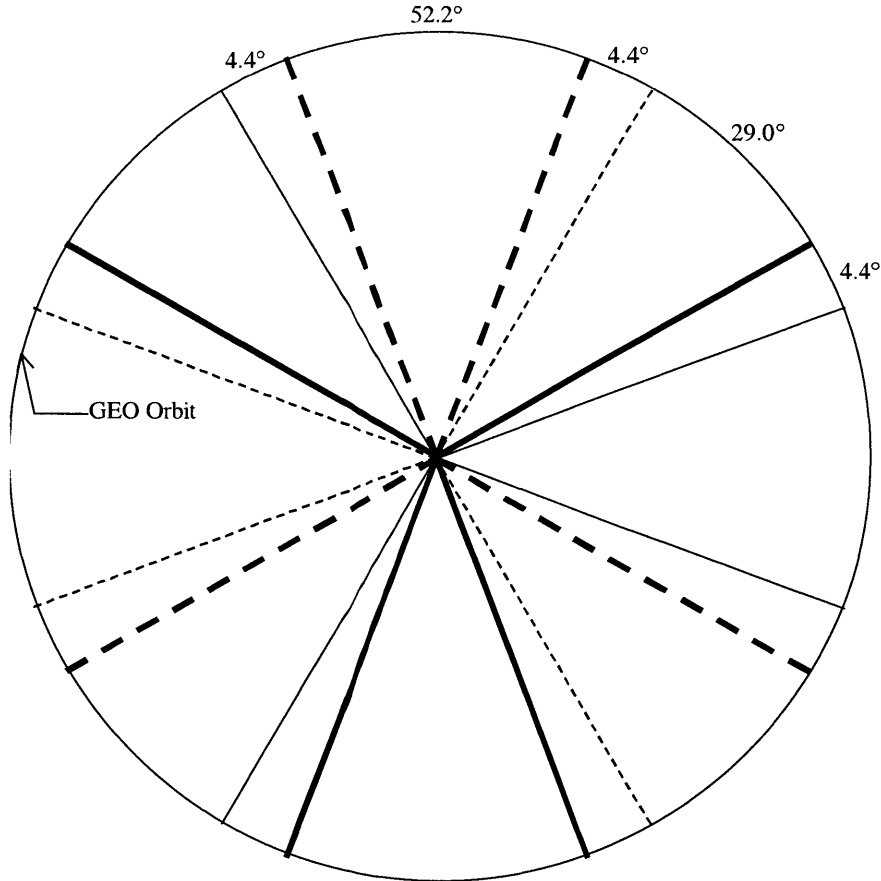
If we wanted only to utilize the earth-facing plane of the backbone satellite, however, the region of visibility is reduced. We must subtract out $\cos^{-1}\left(\frac{re + 15{,}000}{re + 35{,}786}\right) =$ 59.5° from each semi-circle of the GEO orbit, meaning that the visibility is now reduced to two 94.5° portions of the GEO plane which are reflections across the plane of the polar MEO orbit. We will consider these two regions to constitute the coverage provided any satellites experiencing obscuration.

We now consider the service provided by the MEO constellation on the GEO orbit plane. If we consider a single polar orbit with 4 evenly spaced MEO backbone satellites, the satellites are separated from each other by 90°. This implies that in the worst case, all four satellites in a MEO backbone satellite plane will experience some obscuration. The

first two of these satellites experience obscuration on one side of earth and the other two satellites on the other side of the earth. Thus, we consider the two sets to both be at the equatorial latitude but directly opposite each other. We model their coverage regions as that bound by the thin solid lines and the thin dotted lines in figure 5-18, with two satellites per coverage region. The second orbital plane, which is perpendicular to the first, adds two more sets of regions, those bound by the thick solid and thick dotted lines. With a bit of calculation, we find each of the small overlap regions to be 4.4°. The top, bottom, left, and right regions are 52.2°, and the diagonal regions are 29.0°, as illustrated on figure 5-18. The 4.4° regions experience 6-fold coverage, while the 52.2° and 29.0° regions experience 4-fold coverage. Thus, the fraction of users for which one backbone satellite is responsible amounts to

$$F_{\text{MEO-GEO}} = \frac{2\left(3 \bullet \dfrac{4.4°}{6} + \dfrac{29.0°}{4} + \dfrac{52.2°}{4}\right)}{360°} = \frac{1}{8}. \tag{5.24}$$

Thus we can see that apertures servicing GEO users can be evenly divided amongst the earth-facing surfaces of all of the MEO backbone satellites.
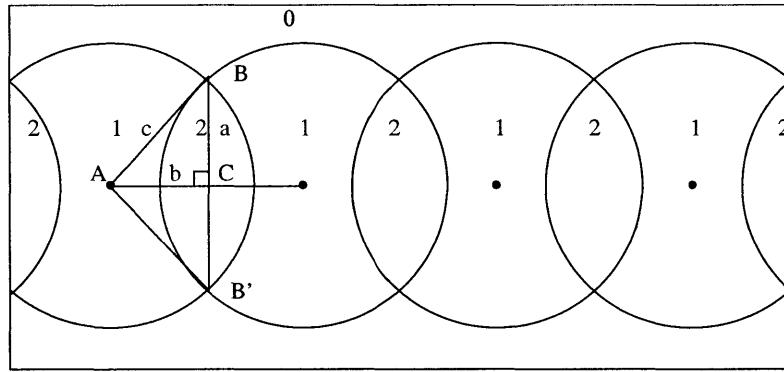
Figure 5-18: The coverage profile of the MEO constellation on the GEO user orbit.

5.3.3.2 MEO Backbone-MEO/LEO User

From equation 1, we have calculated the service radius of a MEO satellite at 15,000 km altitude on the LEO sphere at 250 km altitude to be 88.4°. Because this is nearly 90°, we know that the coverage region of a single backbone satellite is nearly a semi-sphere. Thus, if we consider the service provided by a single MEO plane, which has 4 satellites separated by 90° each, we can visualize that the only holes in coverage are extremely small opposing areas on the user plane's equator 90° away from the intersection of the equator with the orbital tract. We will thus proceed with the analysis of the coverage profile of a single MEO plane to show that the hole in single-planed coverage is insignificant and then make remarks about the optimality of double-planed coverage.

In figure 5-19, we've borrowed the diagram from the GEO case and modified it to suit the need of the MEO case. We must now view the long side of the rectangle as an

entire unrolled polar orbit path and the short side as only one-half of the equator. Also, the circles now indicate coverage regions rather than coverage holes, and the integers indicating the level of service enjoyed by each region has been modified accordingly. However, the spherical geometric identities used to calculate the areas of the service regions still apply, and we use them again here.

Figure 5-19: A rectangular projection of the coverage profile of one plane of the MEO backbone on the 250 km LEO sphere.

We first find the area of each spherical circle to be $6.11R^2$ using equation 5-9. We also know that side c is equal to $88.4°$ from the coverage equation and that side b is equal to $45°$, one-half of the separation between the satellites. We also know that angle C is $90°$ because a segment joining the intersections of two circles and a segment joining their centers must be perpendicular. With the spherical law of sines (5-10), we find that angle B is $45.02°$. We then find angle A to be $88.39°$ using equation 5-11. This then tells us the area of the pie-slice BAB' is

$$A_{pie} = \frac{2(88.39)}{360} 6.11R^2 = 3.00R^2. \qquad (5.25)$$

The triangle BAB' has area $2\pi R^2(88.39+45.02+90-180)/180$, which is $1.515R^2$. This means that the double coverage section has area

$$A_{double} = 2R^2(3.00-1.515) = 2.97R^2 \qquad (5.26)$$

and that the single coverage section has area

$$A_{single} = 6.11R^2-2(2.97R^2) = 0.17R^2. \qquad (5.27)$$

We can use these two values to compute the area covered by a single MEO plane, which is

$$A_{plane} = 4(A_{single}) + 4(A_{double}) = 12.56R^2. \tag{5.28}$$

The entire area of the sphere is $4\pi R^2$, which is about $12.5664R^2$, meaning that a single MEO orbit can cover approximately 99.95% of the 250 km altitude LEO user sphere, with the miniscule holes in coverage occurring around 90° from the sub-satellite points, or exactly on the path traced out by the sub-satellite points of the second plane, meaning that they are certain to be covered. Since it provided by just a single plane, this coverage is also not subject to variation in time, thus we do not have to worry about "worst-case" situations occurring for an individual satellite.

Let us now consider the fraction of the users for which a single satellite would be responsible given only one backbone plane. We know that it provides single coverage for an area of $A_{single} = .17R^2$ and shares coverage with another satellite over $2A_{double} = 2(2.97R^2)$. This means that the fraction of users it is responsible for is

$$\frac{.17 + \frac{2(2.97)}{2}}{4\pi} = .2499, \tag{5.29}$$

which is nearly ¼ of all of the users, with the slight difference resulting from the coverage gaps. We can safely estimate that outside the minute gaps, a single MEO plane can provide maximally efficient coverage of the portion of the 250km LEO sphere to which it is visible. With two planes, the MEO constellation easily covers the any gaps, and we also know that covering the small gaps will hardly contribute a significant portion of users to any one plane's load. Thus, we can conclude that with two planes, a MEO backbone constellation can provide maximally efficient coverage of the 250km LEO sphere and, as we previously argued, the entire space of LEO and MEO users.

5.3.3.3 Apertures for Handoffs
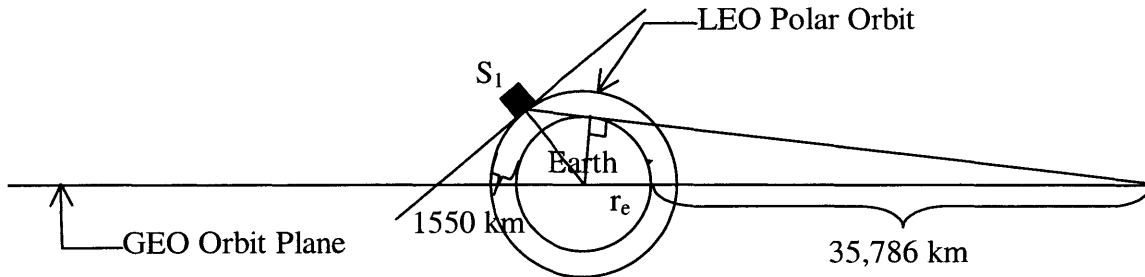
Regarding handoffs, we know that >99.5% of the space of all users will experience coverage by at least 2 backbone satellites at all times, if not by more, simply due to the overlapping coverage areas of the planes. We also know that the contiguous coverage region that a MEO satellite provides is at least ¼ the size of the GEO plane and also at least ½ the size of the LEO/MEO user spheres. Multiple levels of coverage over large

72

contiguous coverage regions allow a large amount of time for each handoff, on the order of up to half a user orbital period. Thus, we can safely conclude that each backbone satellite need only carry 1 more aperture in order to accomplish make-before-break handoffs. Our MEO backbone constellation is thus completely optimal in terms of aperture assignment, just as our GEO backbone constellation was.

5.3.4 LEO Backbone

5.3.4.1 LEO Backbone-GEO User

We now analyze the coverage that a single LEO backbone provides to the GEO orbit ring, in much the same manner as our MEO analysis was conducted. For a polar plane of LEO backbone satellites, full visibility of the GEO orbit plane occurs at

Figure 5-20: The visibility of the GEO orbit plane from a LEO polar orbit.

$$180° - \cos^{-1}\left(\frac{r_e}{r_e + 35,786}\right) - \cos^{-1}\left(\frac{r_e}{r_e + 1550}\right) = 62.3° \qquad (5.30)$$
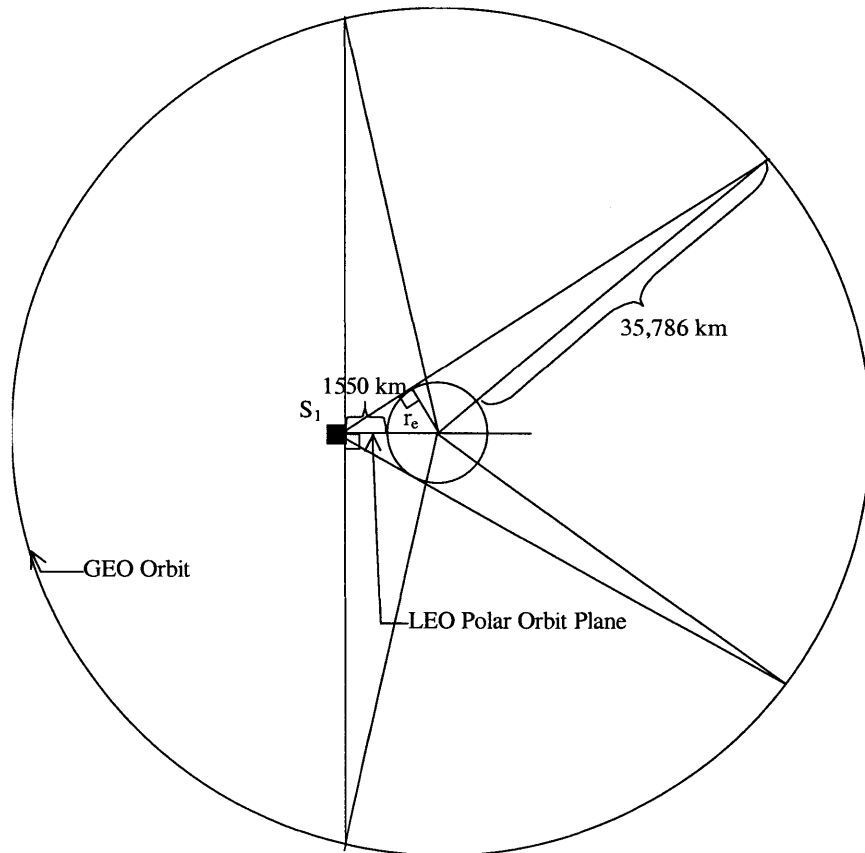
past the equatorial plane. In order for us to utilize only the bottom surface for apertures, however, full visibility occurs at $\cos^{-1}\left(\frac{re + 1550}{re + 35,786}\right) = 79.2°$ past the equatorial plane, meaning that only for two 20° window near the poles will the LEO satellites be able to service all of the GEO backbone. Since 45° separate each satellite in a 8-satellite LEO plane, in the worst case, all of the LEO satellites in one plane will undergo obscuration by the earth.

When a LEO backbone satellite is at the equator, it experiences the maximum obscuration by the earth, which renders

$$2*(180° - \cos^{-1}\left(\frac{r_e}{r_e + 35,786}\right) - \cos^{-1}\left(\frac{r_e}{r_e + 1550}\right)) = 124.6° \qquad (5.31)$$

of the GEO orbit invisible to it. Thus, at least 235.4° of the GEO orbit are visible to a LEO satellite at all times.

If we wanted to use only the bottom surface of the LEO satellite for service, however, then we must subtract out $\cos^{-1}\left(\frac{re + 1550}{re + 35,786}\right) = 79.2°$ from each half of the service region, leaving two regions of 38.5° as the region serviced by each LEO satellite. Figure 5-21 illustrates the basis for these calculations. Thus, we will model the coverage region of every LEO backbone satellite experiencing obscuration to be two 38.5° regions which are reflections across the orbital plane and are separated from each other by 124.6°. These regions are illustrated to scale in figure 5-22 as the regions bound by the boldest lines with angle measurements between them.
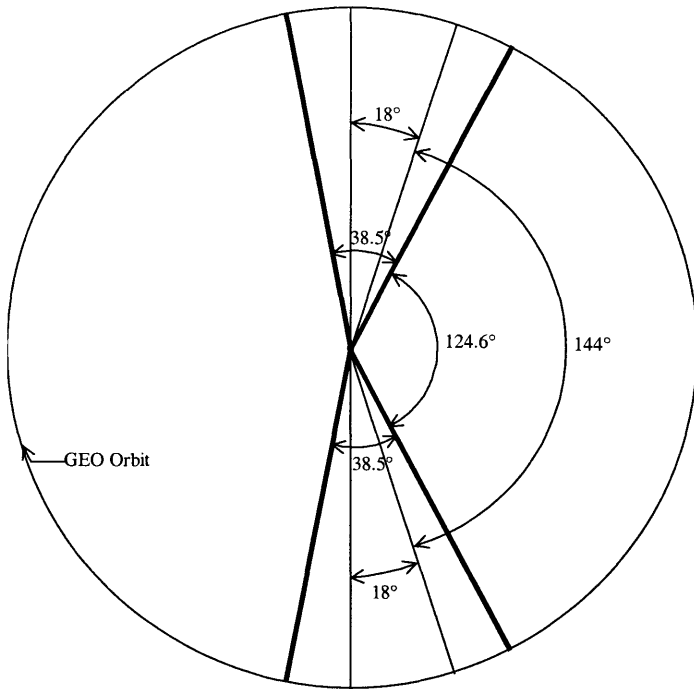

Figure 5-21: Service region provided on the GEO user orbit by a LEO backbone satellite using only its earth-facing surface.

74

Now, we can freely assign a backbone satellite to cover only the users within a certain sub-region of its region of visibility. For reasons which will soon be apparent, we will require that a backbone satellite only cover the regions of the GEO plane between the thinner lines, i.e. two 18° regions sharing a diameter as one border and with their other borders separated by 144°.
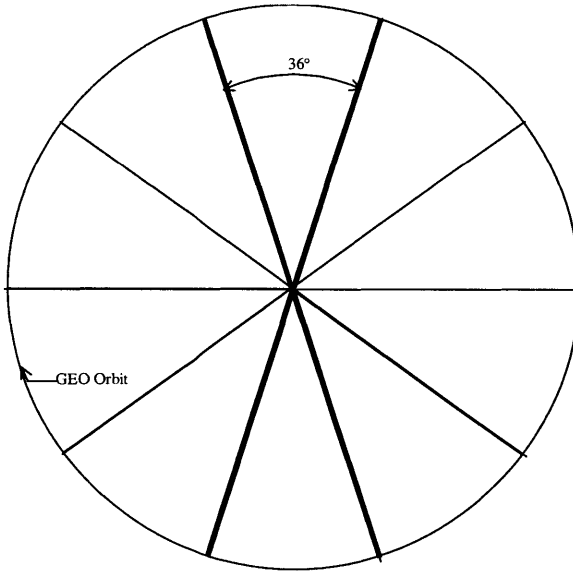
The 8 satellites in the same orbital plane can be split in half, with 4 satellites on one side of the earth and 4 on the other side. Thus, the coverage region of an entire plane is as shown in bold in figure 5-23, with two opposing 36° regions sharing two lines as their boundaries. When this region is replicated five times with a rotation of 72° between each replication, we see that it exactly covers the 360° GEO user circle with no overlapping regions. In order to achieve this coverage, each satellite is responsible for 36° of the plane, with each 36° region experiencing 4-fold coverage. Thus, each satellite is responsible for

$$F_{LEO-GEO} = \frac{\frac{36}{4}}{360} = \frac{1}{40} \qquad (5.32)$$

of the users, demonstrating that the LEO backbone distribute the coverage of the GEO user plane in a maximally efficient manner.

Figure 5-22: The coverage region of a single LEO backbone satellite experiencing obscuration from the earth on the GEO user orbit. The actual limits of visibility are marked in bold, while the coverage region used to prove optimal aperture division is bound by regular lines.


Figure 5-23: A designed coverage profile of the LEO backbone constellation on the GEO user orbit

5.3.4.2 LEO Backbone-MEO/LEO user
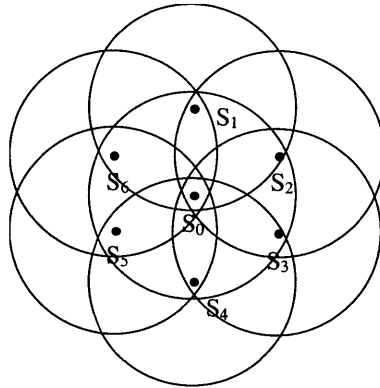
We must now consider the case of a LEO backbone servicing MEO and LEO users. Here is another case where the user are distributed in spherical spaces and the backbone satellites are in polar orbits, like the MEO backbone-MEO/LEO user case. Thus, we must first examine the lowest user sphere, at 250 km altitude, to determine if maximally efficient coverage is feasible. In the case of the LEO backbone, with 5 planes of 8 satellites each, it is difficult to analytically compute the full coverage profile with all of the intersections and regions. Instead, we shall use an engineering estimate to argue for the infeasibility of maximally efficient coverage provided by the LEO backbone.

We know that in order to provide maximally efficient coverage, each backbone satellite must be responsible for an equal and minimal amount of users at all times. For the 40-satellite LEO constellation, this means that each satellite can be responsible for no more than $1/40^{th}$ of all of the users at one time. Assuming that each backbone satellite services all of its "visibility region," which is great in size than $1/40^{th}$ of the entire 250km LEO sphere, over its whole orbit, we know that there must be multiple levels of coverage on these regions at all times in order for the backbone satellite to be able to "share coverage" with follow backbone satellites and achieve this maximally efficient service. Indeed, this is how the MEO backbone constellation, in which the visibility region of each backbone satellite is nearly ½ of the 250km user sphere, achieves maximally efficient coverage. We will see that this cannot be the case for the LEO backbone, however. On the 250 km altitude LEO user sphere, the 1550 km LEO backbone satellite has a service region with radius 51.7°. This service region has area

$$2\pi R^2(1-\cos(51.7°)) = 2.389R^2. \tag{5.33}$$

This is $\dfrac{2.389}{4\pi}$ = .19 of the whole sphere. Thus, if the entire visibility region of a LEO backbone satellite were single coverage, a single backbone satellite would be responsible for .19 of all the users, which is obviously not optimal. In order to achieve optimality, a LEO backbone satellite must average a service level of $\dfrac{.19}{\frac{1}{40}}$ = 7.6 fold over its coverage region at all time over its orbit. This number, however, is unachievable, since a satellite only has 6 nearest neighbors, as shown in figure 49. Thus, if all neighboring satellite's

coverage region covers S_0's sub-satellite point, we then have a region of seven-fold coverage around the sub-satellite point of S_0. This is indeed the case for the LEO backbone, since the distance between backbone satellites within the same plane is only 45°, and the distance to the nearest satellites in the neighboring planes also does not exceed 51.7°, the coverage radius of one satellite. As an aside, this allows us to use only one additional aperture per backbone satellite to achieve make-before-break handoff, since it demonstrates the large regions of multiple coverage in the LEO coverage profile, thus allowing for a long time period in which to schedule hand-offs.[1]

Figure 5-24: The six nearest neighbors of satellite S_0.
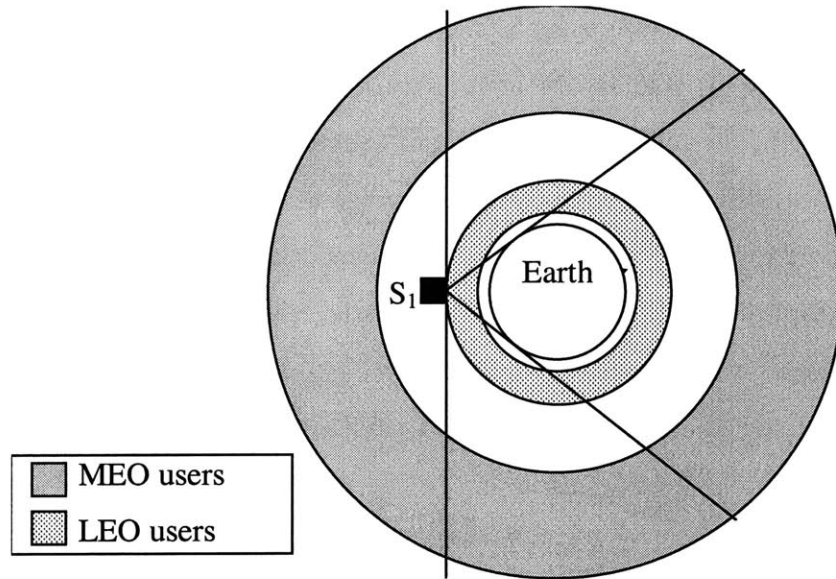
While seven-fold coverage exists for the LEO backbone constellation, averaging a coverage level of 7.6 requires large regions where the coverage level is in excess of seven. This extra coverage cannot come from satellites within the same plane, since their distance to each other always remains fixed. The next nearest satellites other than the ones pictured are two planes away with the same phase angle as S_0. While S_0 is near the equator, however, those satellites are 72° away from S_0, since there are a total of five orbital planes. They are too far to cover S_0's sub-satellite point. Thus, in the worst-case equatorial regions, S_0 would not be able to a achieve 7.6-fold coverage and would thus be responsible for providing service to more than 1/40th of the users at that time, thus

---

[1] As an aside, this allows us to use only one additional aperture per backbone satellite to achieve make-before-break handoff, since it demonstrates the large regions of multiple coverage in the LEO coverage profile, thus allowing for a long time period in which to schedule hand-offs.

requiring it to carry more apertures. Hence, we know that a LEO backbone constellation cannot provide maximally efficient service to LEO/MEO users.

A LEO backbone satellite contains one additional deficiency in its provision of user-access apertures. Figure 5-25 diagrams how a LEO would provide service to the LEO/MEO sphere.


Figure 5-25: The service area of a LEO backbone satellite on the MEO and LEO user spheres.

We can see that the LEO backbone satellite can provide service for all of the LEO users by just using the earth-facing surface of the satellite. In order to provide service for all of the MEO regions to which it is visible, however, the LEO backbone satellite must utilize both the earth-facing surface and the "space-facing" surface. The lack of apertures on that "space-facing" surface would remove a circle of radius $\cos^{-1}\left(\dfrac{re+1550}{re+5000}\right)=45.8°$ from the service region of a LEO backbone on the lowest MEO user sphere. The service region has a radius of $\cos^{-1}\left(\dfrac{re}{re+1550}\right)+\cos^{-1}\left(\dfrac{re}{re+5000}\right)=92.3°$, so this removal results in a loss of about 30% of the service region, a significant portion. So, the LEO backbone satellite must carry apertures on its "space-facing" side to avoid this loss. The location of these apertures prevent them from being used to service for LEO users, whereas on MEO and GEO backbone satellites all apertures can be used to service users of all three classes.

These apertures must be considered "extra" apertures used for filling in the gaps in the MEO coverage region. The presence such apertures introduces an inefficiency into the aperture assignments, since we must also provide apertures on the earth-facing service for MEO users, because the majority of the MEO coverage area for a backbone satellite still faces that side. While it may be theoretically possible for us to decrease the number of apertures facing earth because some MEO users are served by apertures facing away from earth, we still must provide earth-facing apertures in order to serve a majority of MEO users. Because of the large number of LEO backbone satellites (40) and the relatively small number of MEO users (~20-30), we can handle all MEO user conditions with one space-facing and one earth-facing aperture on each backbone satellite. But this represents 80 apertures for only 20-30 users, and only the 40 earth-facing apertures can also be used to service other user altitude classes. The service gap has caused us to introduce an large number of excessive apertures into the entire satellite system. Thus, we can conclude that the LEO constellation suffers a disadvantage in terms of the efficiency of aperture-to-user assignment when compared to the MEO and GEO constellations.

Chapter 6

Cost Analysis

We have seen that both the MEO and GEO constellations can distribute apertures for user support in a maximally efficient manner, while the LEO constellation suffers some inefficiencies. However, despite their importance, apertures are only a part of the entire satellite communications system. In order to gain a fuller understanding of how our candidate constellations compare to one another, we must now estimate their whole system cost using a speculative cost model. We will center this model around the communications links of the system, certainly, but we also include such fixed costs as the body of the satellite and the launch costs. We begin by introducing the cost equation of our cross-links and proceed by dividing the costs of the entire system into our familiar classifications of the cross-links.

6.1 Cost Equation

The cost of an optical cross-link has been previously modeled in [6] as a function of distance and data rate to be

$$C_{\text{optical}} = k_0 + k_1 R^{\frac{\alpha}{4}} d^{\frac{\alpha}{2}} \tag{6.1}$$

where k_0 is the fixed cost of an optical link, k_1 is the coefficient associated with the variable cost of a cross-link, R is the data rate required over the link, d is the distance of the link, and α is an exponential factor between 2 and 3. Because of the high rate nature of our communications, we will project every cross-link in our system to be optical and thus use this equation to model the
cost of every link.

6.2 Cost Coefficients of Satellite Links

In the cost analysis of a cross-link, we need to define the cost coefficients k_0 and k_1, which are applied to the fixed and variable costs of a cross-link respectively, and also the exponent α. In [6], α was set to 3 and three sets of k_0 and k_1 were defined.

1. $k_0 = 1.000 \times 10^3$, $k_1 = 5.654 \times 10^{-9}$

2. $k_0 = 5.000 \times 10^5$, $k_1 = 4.243 \times 10^{-9}$

3. $k_0 = 1.000 \times 10^6$, $k_1 = 2.828 \times 10^{-9}$

all of which yield a cost of 2 million dollars for a link of 10Gbps with a range of 50,000 km. The first set represents a situation where the fixed cost contributes minimally to the cost of the aperture, while third set represents a situation where fixed cost is predominant. The second set is a medium between the other two. We will utilize these coefficients in our cost analysis.

6.3 User-Access Links

6.3.1 Cost Parameters

The first type of communications links in our system is the user-access link, which occurs between the user and a backbone satellite. If a satellite constellation can support users optimally, the number of such links in the whole constellation is very close to the number of projected users in the systems, plus one extra link per backbone satellite for hand-offs. The exact equation for the number of links required given an optimal distribution is

$$L = T\left(\left\lceil \frac{u}{T} \right\rceil + 1\right) \tag{6.2}$$

where T is the number of backbone satellites in the system and u is the number of users in the system. This equation applies for the GEO and MEO systems. Assuming 100 users in the system, GEO requires 105 apertures and MEO requires 112.

For a non-optimal system like LEO, we must project the exact number of user-access apertures required. We know that the LEO constellation requires apertures facing away from the earth in order to fill in the service gap in the MEO region. As said in the previous section, one such aperture is enough to handle this task. As calculated in the

pervious section, around 30% of the MEO users will be handled by these apertures. The other 70% of MEO users must be serviced by the downward-facing apertures, which also service the other user altitude classes. We must also remember the single aperture required for hand-off. Thus, the number of links required for a LEO constellation is

$$L_{LEO} = T\left(\left\lceil \frac{.7m + (u - m)}{T} \right\rceil + 2\right) \tag{6.3}$$

where T and u are as before and m is the number of MEO users. For a total of 100 users and with 25 MEO users, this yields 200 total apertures in the LEO system. For all of the rest of our analysis, we will assume that MEO users make up 25% of all of the users. This makes our equation

$$L_{LEO} = T\left(\left\lceil \frac{.925u}{T} \right\rceil + 2\right) \tag{6.4}$$
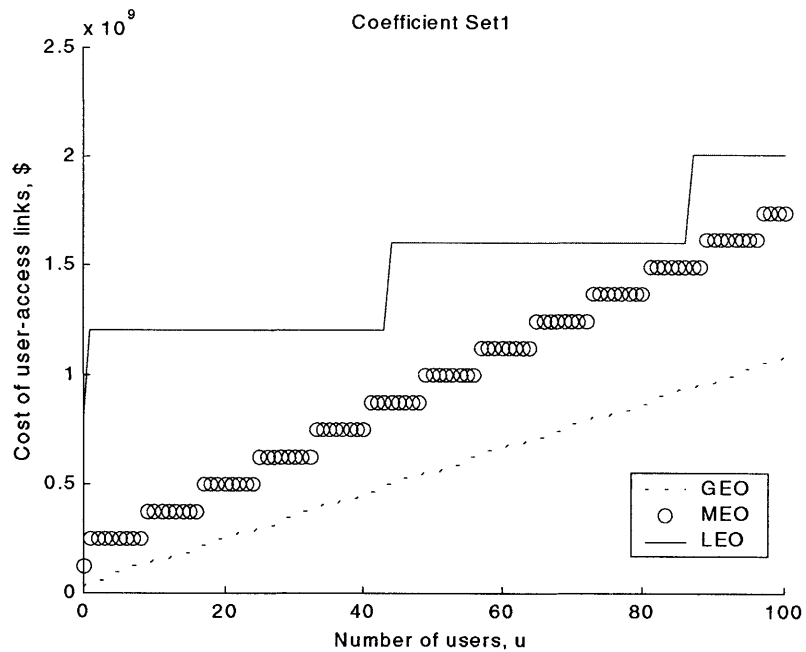
For each user, we must provide for the maximum possible requested rate, which was projected to be 100Gbps. We must also provide this maximum rate at the maximum projected link distance, which was determined for each constellation in a previous section. Thus, for a given set of constant coefficients and exponents, the cost of each user-access link is actually fixed. Thus, the total cost of all of the user-access links in the system is actually only dependent upon the number of users in the system. Thus, we will consider the contribution of user-access links to the cost of the constellation to be only a function of the total number of users. We list the parameters which contribute to this cost for each constellation in the table below.

Constellation	GEO	MEO	LEO
Total no. of apertures as a function of u	$3\left(\left\lceil \frac{u}{3} \right\rceil + 1\right)$	$8\left(\left\lceil \frac{u}{8} \right\rceil + 1\right)$	$40\left(\left\lceil \frac{.925u}{40} \right\rceil + 2\right)$
Maximum data rate of link	100Gbps	100Gbps	100Gbps
Maximum link distance	47,273 km	62,083 km	46,388 km
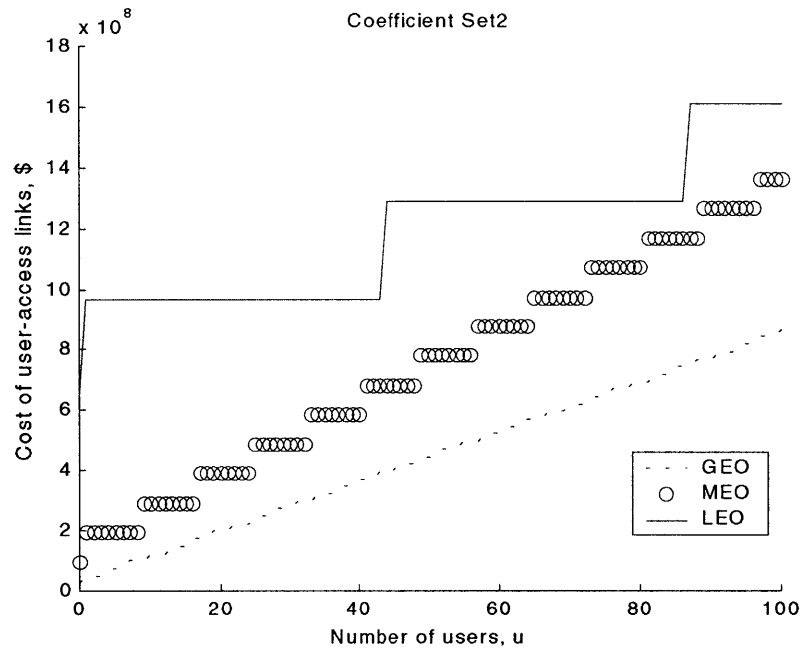
Table 6-1: Cost Parameters of User-Access Links

6.3.2 Numerical Examples of User-Access Link Cost
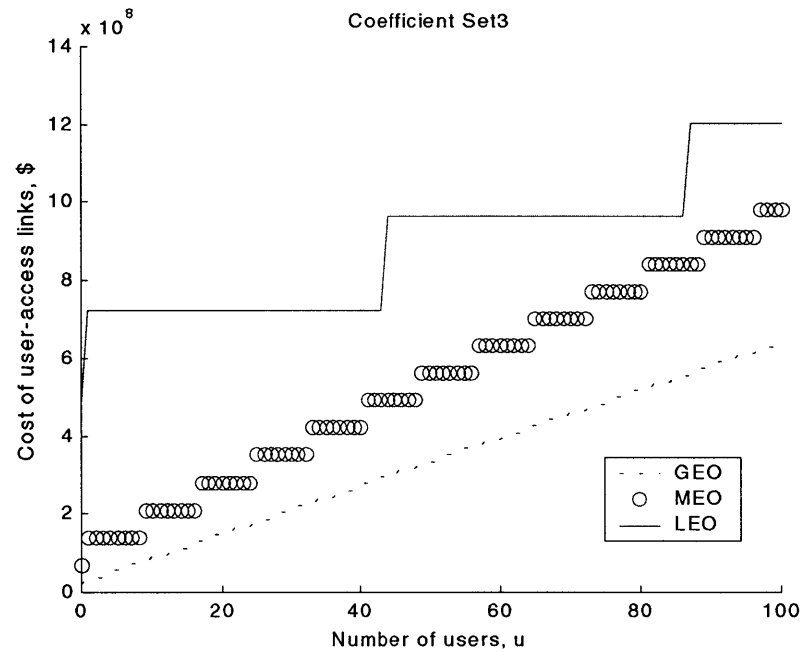
We can now plot some numerical examples of user-access link cost for each type of constellation. Each of the following plots are the costs for all of the user-access links of the entire constellation, not just for each satellite, as a function of the number of users. The total cost of the user-access links in the system equals the total number of apertures in the system times the cost of each individual link. The results are shown below.


**Figure 6-1:** **Cost comparison of system-wide user-access links for the first coefficient set (k_0 = 1.000×10³).**

Figure 6-2: **Cost comparison of system-wide user-access links for the second coefficient set ($k_0 = 5.000 \times 10^5$).**


Figure 6-3: **Cost comparison of system-wide user-access links for the third coefficient set ($k_0 = 1.000 \times 10^6$).**

6.4 Intra-Backbone Links

6.4.1 Cost Parameters

Intra-backbone links are the cross-links which occur between a pair of backbone satellites. We will now proceed in much the same fashion as we did for user access links to find the parameters which contribute to the cost of the constellation's backbone links.

First, we know that most polar satellite constellations are implemented with four backbone cross-links per satellite, two being intra-plane and one to the nearest neighboring planes east and west. This is what we will assume for the MEO and LEO constellations. For the GEO constellations, however, we will assume the presence of only two cross-links per satellite, since the GEO is only a planar constellation.

We have also already calculated the maximum distance of the cross-link for all constellations in a previous section. Thus, the only significant parameter left to determine is the data rate capacity required for each link. We will rely heavily on [6] for this calculation and utilize the uniform traffic assumption introduced there. Under this assumption, there is a total level of traffic T_u in the entire system, and the same amount of traffic originates from each backbone satellite. The traffic originating from one backbone satellite is also sent equally to all backbone satellites, including itself. Thus, each backbone-backbone pair (including duplicates) of source-and-sink contains an equal amount of traffic. We will also model T_u as a function of the total number of users in the system, with a minimum of $10u$Gbps and a maximum of $100u$Gbps.

With this assumption, we can enumerate nine such different pairs for the GEO constellation. Assuming shortest-path routing, which makes each source-sink path either one or zero hops, we easily find that each intra backbone cross-link is responsible for two of the nine pairs. Thus, for GEO, we know that the maximum capacity required of each cross-link is $\frac{2}{9}T_u$.

With MEO and LEO, we utilize the seamed network modeled described in [6], which tells us that the data-rate capacity required for both inter-plane and intra-plane cross-links is $\frac{T_u}{8M}$, where M is the number of planes in the backbone constellation. Thus,
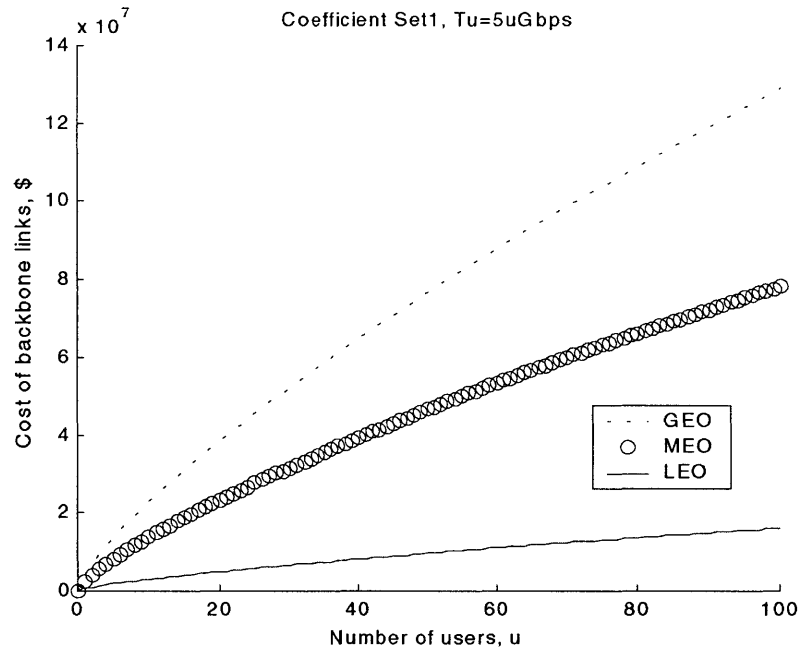
for MEO, the capacity required is $\frac{T_u}{16}$, and for LEO, the capacity required is $\frac{T_u}{40}$. The table below summarizes the parameters which determine cost for the intra-backbone cross-links in the system.

Constellation	GEO	MEO	LEO
Total no. of apertures	$3 \bullet 2 = 6$	$8 \bullet 4 = 32$	$40 \bullet 4 = 160$
Maximum data rate of link as a function of T_u	$\frac{2}{9}T_u$	$\frac{T_u}{16}$	$\frac{T_u}{40}$
Maximum intra-plane link distance	73,030 km	30,233 km	6,068 km
Maximum inter-plane link distance	N/A	32,371 km	5,715 km
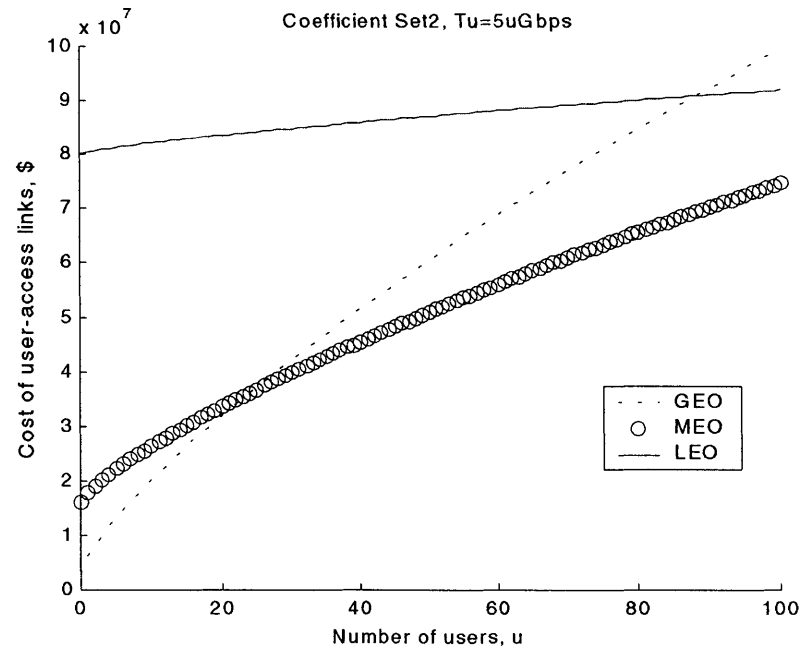
Table 6-2: Cost parameters of the intra-backbone link

6.4.2 Numerical Examples of Intra-Backbone Link Costs
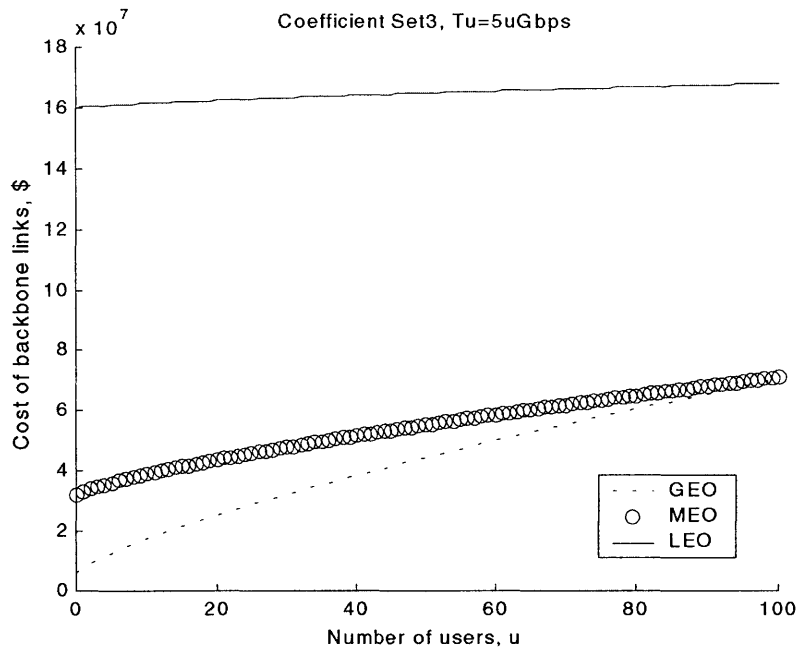
Having established the equation for the cost of all the intra-backbone links of a satellite constellation, we can now compare that cost for the LEO, MEO, and GEO constellations under various circumstances. We will of course utilize the three sets of cost coefficients to represent different contributions of fixed satellite cost as before, but we will now also vary T_u to represent situations of low system traffic, medium system traffic, and high system traffic. We will choose T_u equals $5u$Gbps to represent low system traffic, since this means that the average user demand is only 5Gbps, on the low end of our projections. It then follows that $20u$Gbps represents the T_u for situations of medium traffic demand and $100u$Gbps should represent situations of high traffic demand. These cases affect the data-rate capacity that must be carried by each intra-backbone links. The plots resulting from each situation were generated and are now presented below.
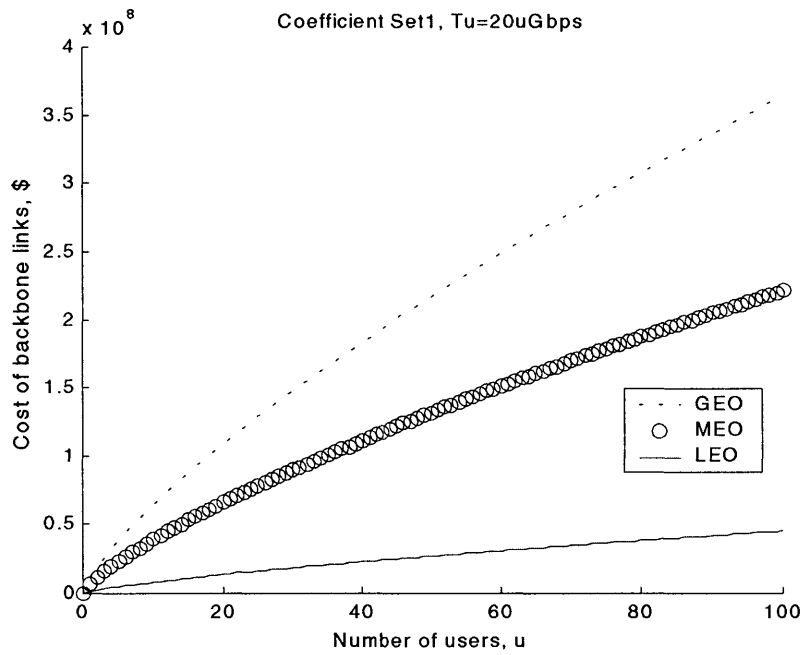
Figure 6-4: Cost comparison of system-wide backbone links for the first coefficient set ($k_0 = 1.000 \times 10^3$) and low traffic conditions
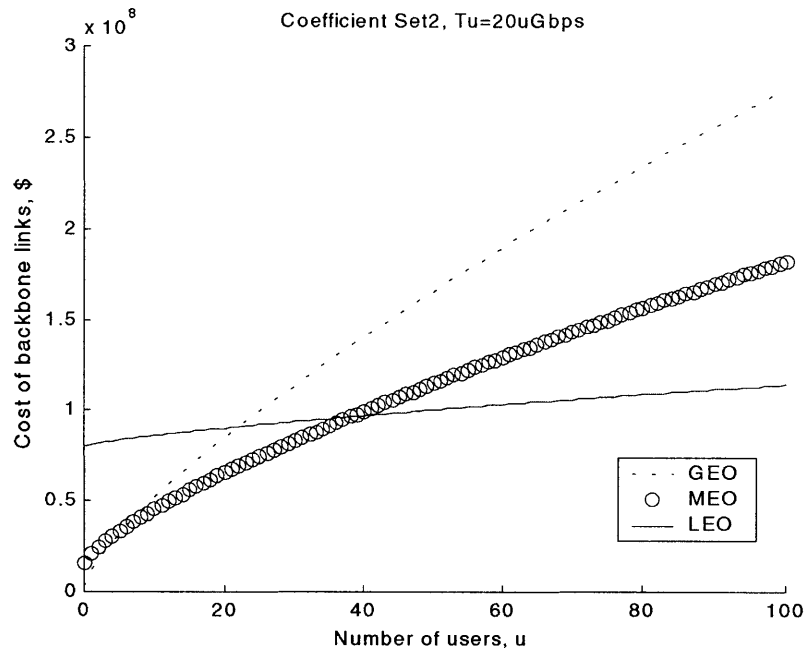

Figure 6-5: Cost comparison of system-wide backbone links for the second coefficient set ($k_0 = 5.000 \times 10^5$) and low traffic
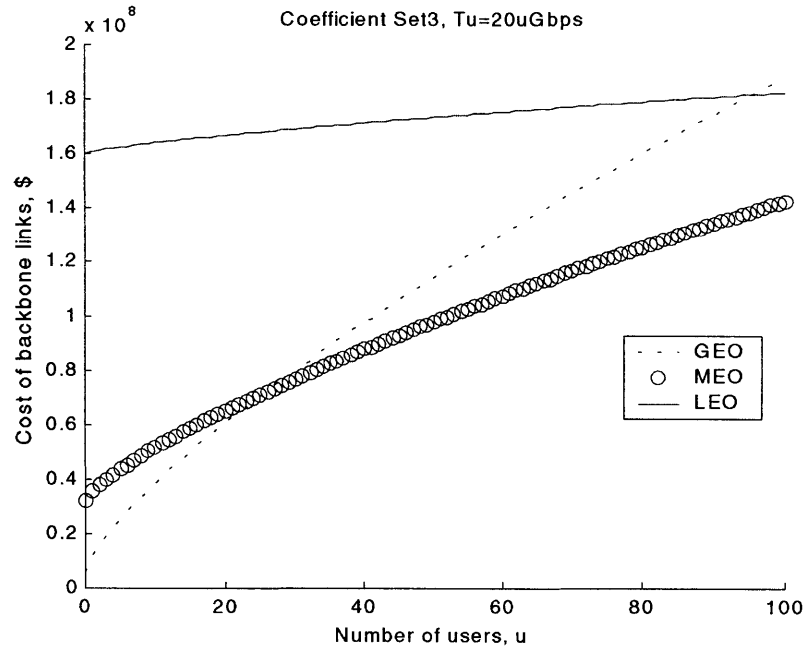
Figure 6-6: Cost comparison of system-wide backbone links for the third coefficient set ($k_0 = 1.000 \times 10^6$) and low traffic
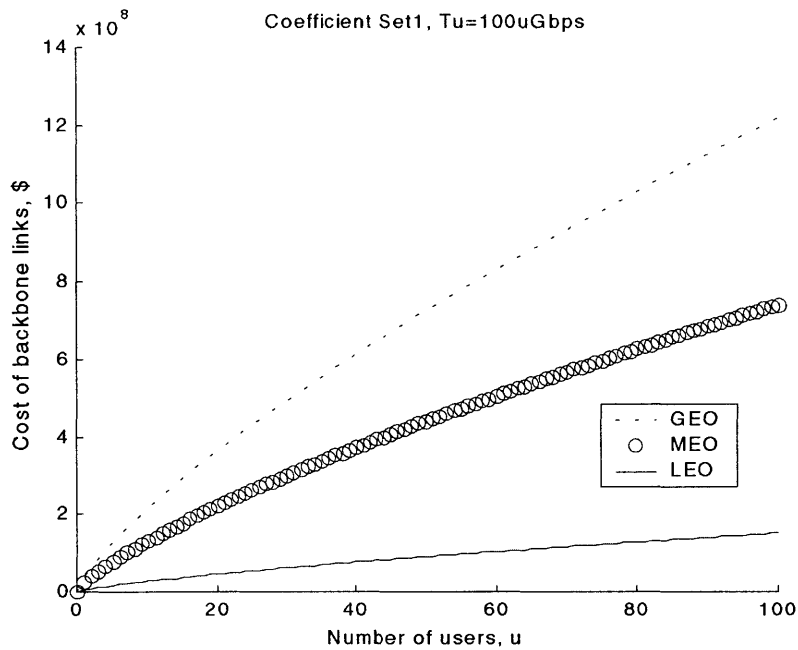

Figure 6-7: Cost comparison of system-wide backbone links for the first coefficient set ($k_0 = 1.000 \times 10^3$) and medium traffic
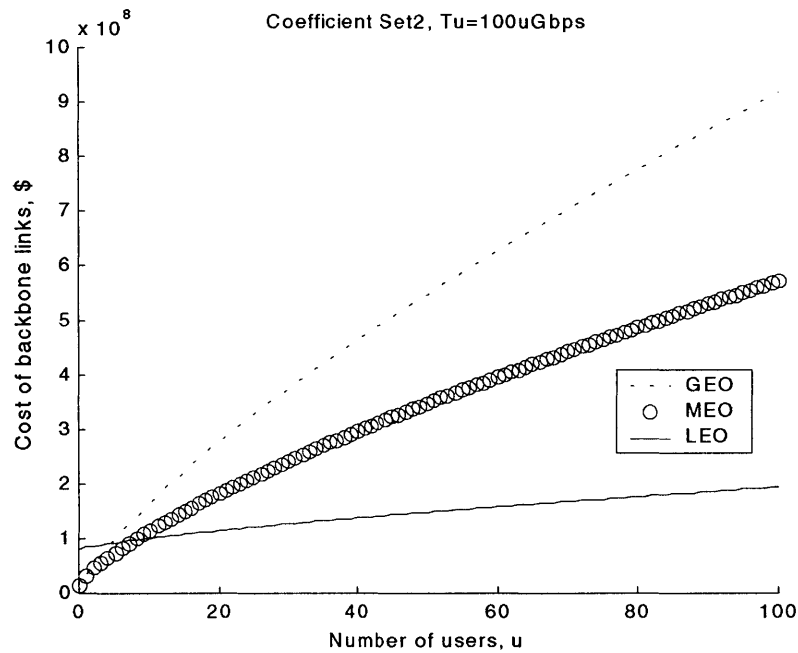
Figure 6-8: Cost comparison of system-wide backbone links for the second coefficient set (k_0 = 5.000×10^5) and medium traffic
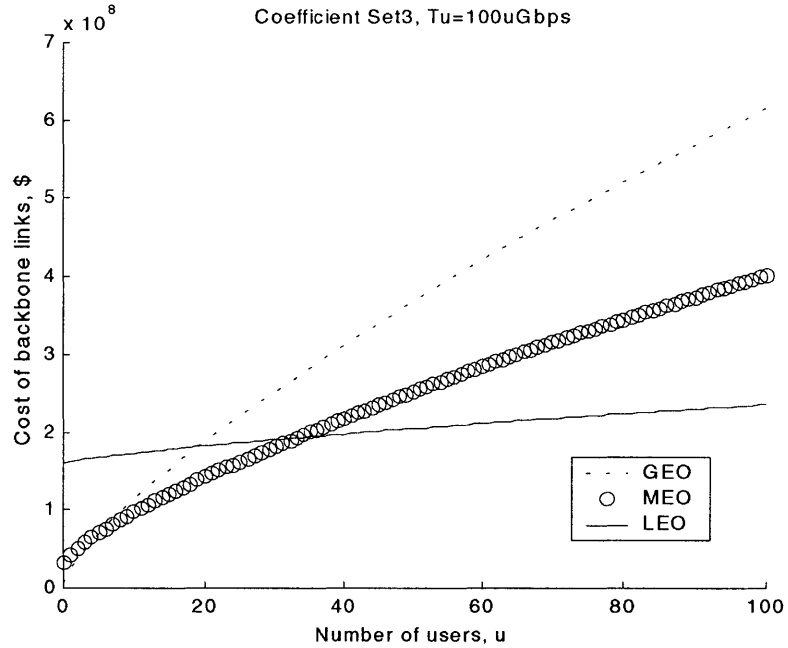

Figure 6-9: Cost comparison of system-wide backbone links for the third coefficient set (k_0 = 1.000×10^6) and medium traffic

Figure 6-10: Cost comparison of system-wide backbone links for the first coefficient set (k_0 = 1.000×10³) and high traffic


Figure 6-11: Cost comparison of system-wide backbone links for the second coefficient set (k_0 = 5.000×10⁵) and high traffic

Figure 6-12: Cost comparison of system-wide backbone links for the third coefficient set (k_0 = 1.000×10^6) and high traffic

6.5 Cost Equation of Entire Constellation

The cost equation of the entire constellation consists of the sums of costs of the user-access links, the backbone-links, the fixed cost of the satellite body, and the launch costs for all of the satellite in the constellation. Although k_0 is the coefficient of fixed cost for the communications link, it can also be used as a sensible estimate for the fixed cost of the satellite body, since it models the cost of supporting the apertures as increasing proportionally with the number of cross-links. As an example, it reasonably models a GEO backbone satellite carrying 30-some user access links and 2 intra-backbone links as having around five times the fixed cost of a LEO backbone satellite with 4 user-access and 4 intra-backbone links. We do not, therefore, need to include a separate constant for the cost of a satellite body.

As for satellite launch costs, NASA's Cost Estimating Group provides data on expendable launch vehicles to orbits of various altitudes [7]. Using data from their web page, we estimate the launch cost of each LEO satellite to be around $30 million, the launch cost of each MEO satellite to be around $150 million, and the launch cost of each
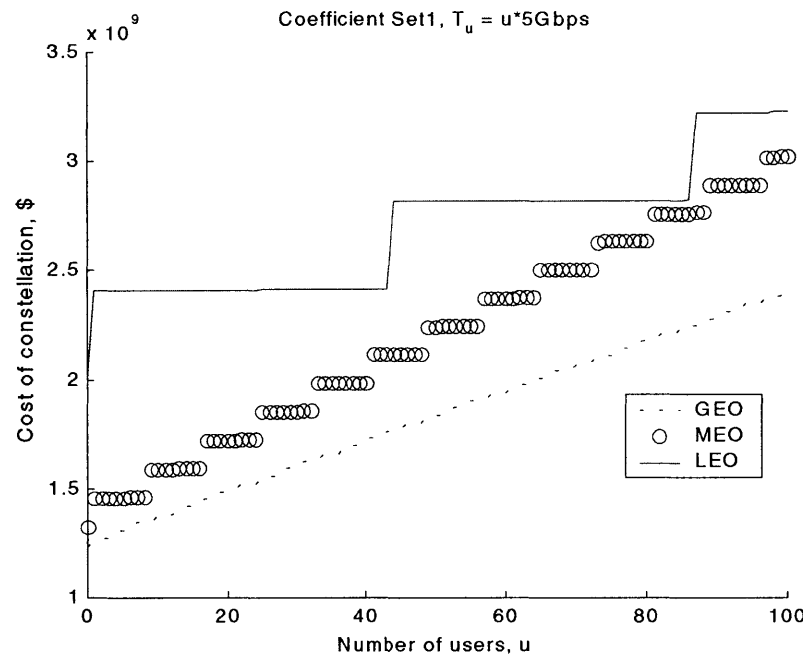
GEO satellite to be around \$400 million. Thus, the final equation for the cost of the entire constellation is

$$C_{constellation} = N_{user\text{-}access\ links} \bullet C_{user\text{-}access\ link} + N_{backbone\ links} \bullet C_{backbone\ link} + C_{launch}, \quad (6.5)$$
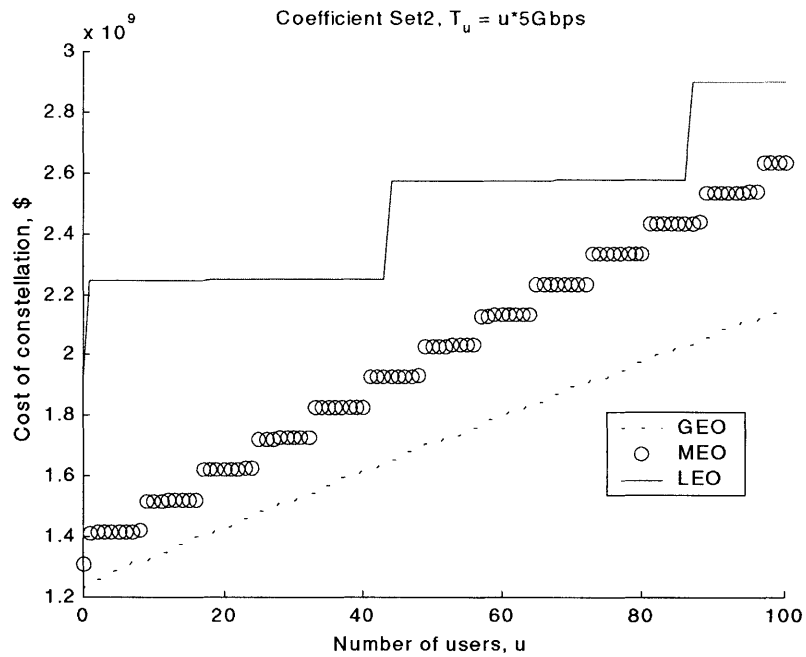
where $N_{user\text{-}access\ links}$ is the number of user-access cross-links and $N_{backbone\ links}$ is the number of backbone cross-links.

6.6 Numerical Examples
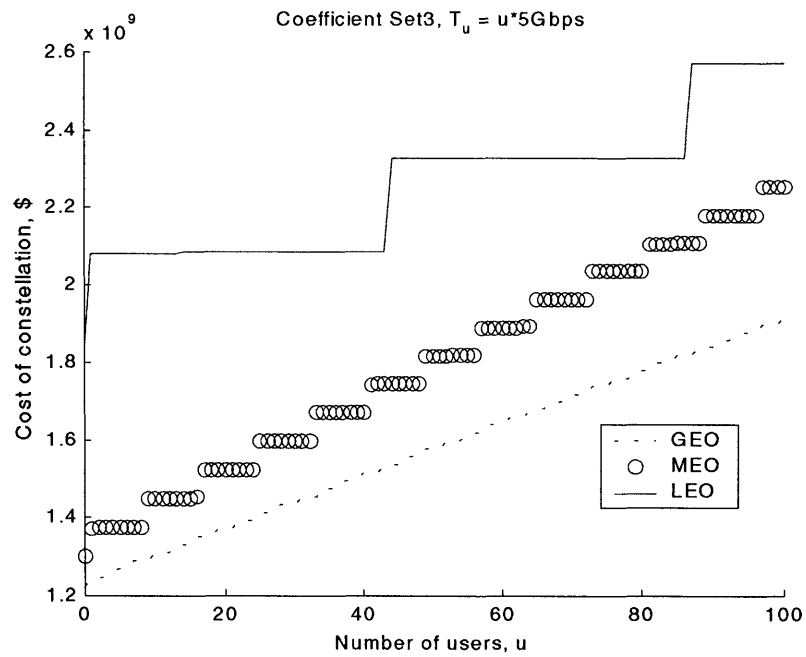
We now add the projected launch costs to our previous cost estimates for the two types of links to produce a final estimate of system cost. There were again nine permutations of three coefficient sets and three traffic conditions. The plots resulting from each permutation are now presented below.
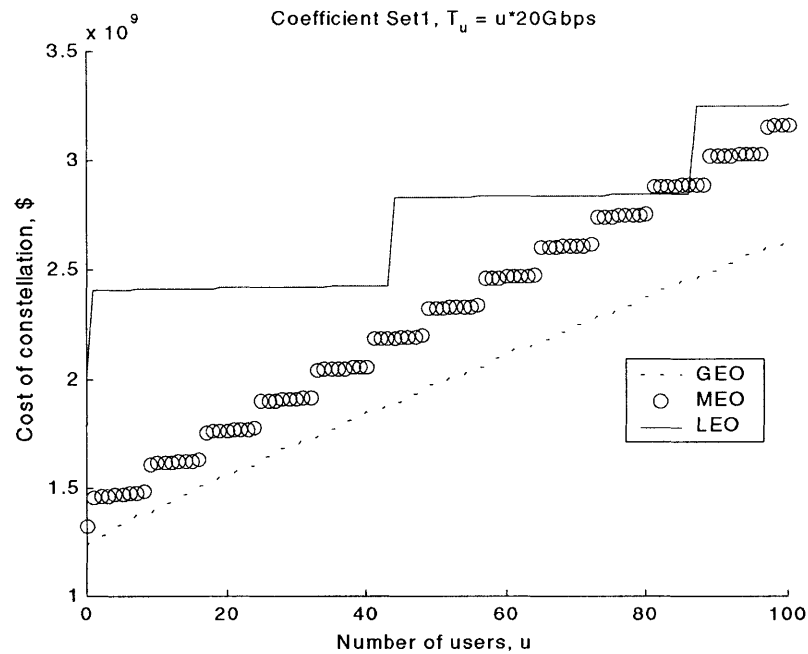
Figure 6-13: Constellation cost comparison for smallest contribution of fixed cost (k_0 = 1.000×10³) and low system traffic

Coefficient Set2, T_u = u*5Gbps
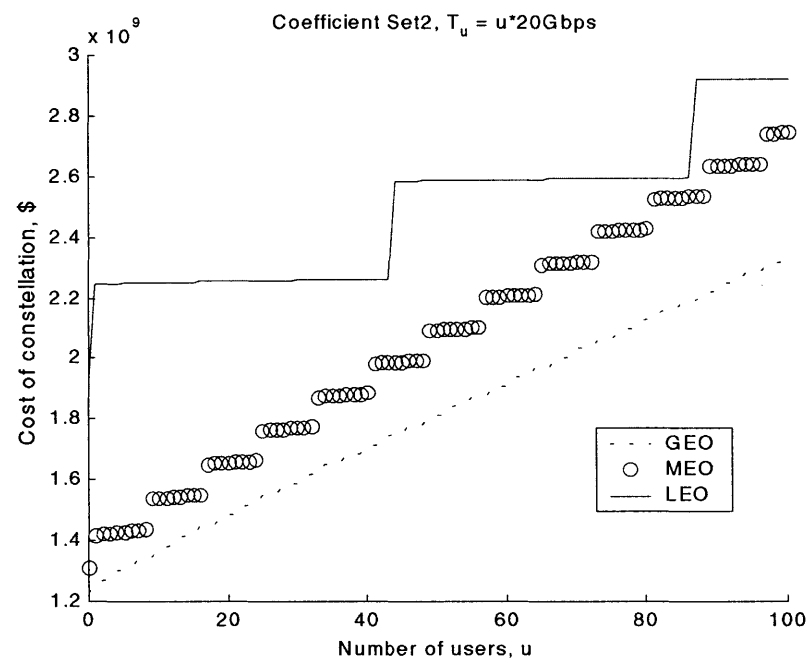
Figure 6-14: Constellation cost comparison for medium contribution of fixed cost (k_0 = 5.000×10⁵) and low system traffic


Coefficient Set3, T_u = u*5Gbps
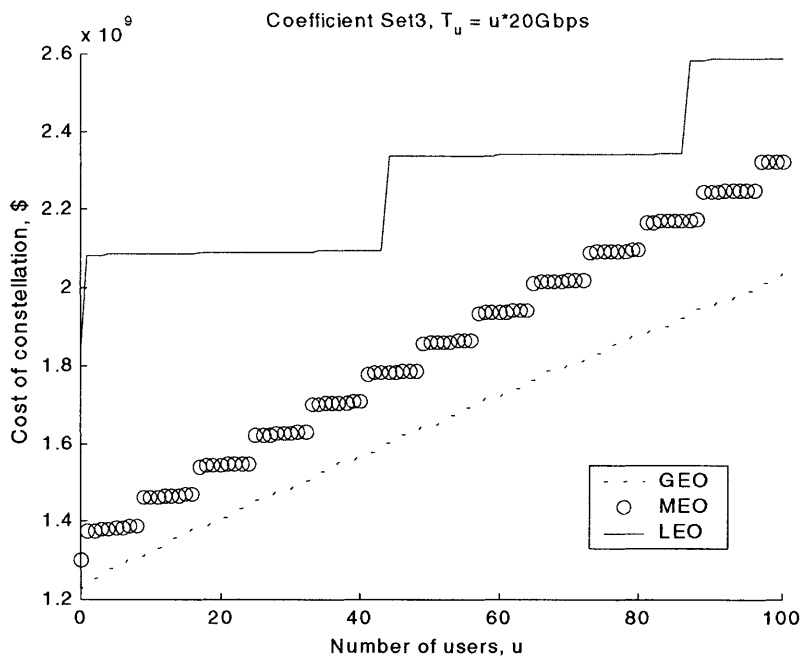
Figure 6-15: Cost Comparison for largest contribution of fixed cost (k_0 = 1.000×10⁶) and low system traffic
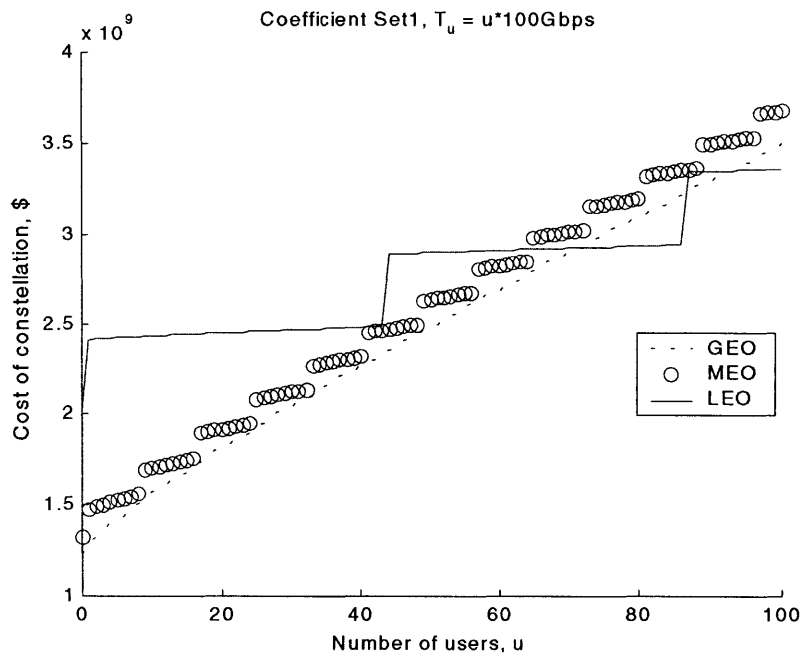
Figure 6-16: Constellation cost comparison for smallest contribution of fixed cost (k_0 = 1.000×10³) and medium system traffic
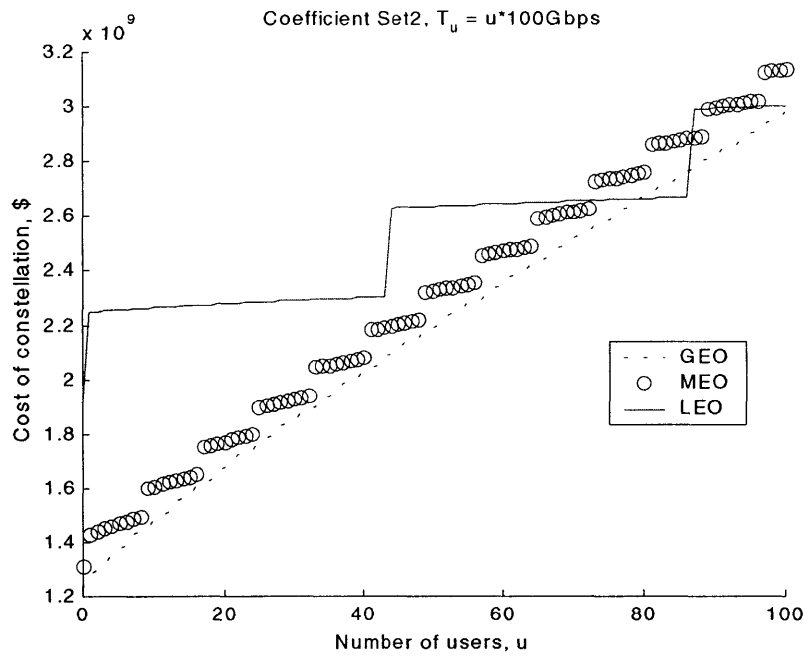
Figure 6-17: Cost Comparison for medium contribution of fixed cost (k_0 = 5.000×10⁵) and medium system traffic
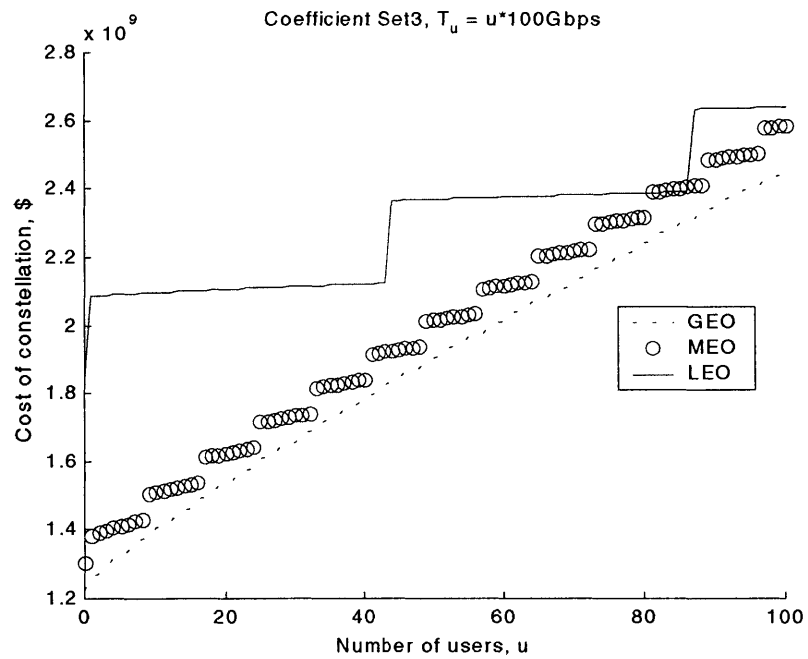
Figure 6-18: Constellation cost comparison for largest contribution of fixed cost (k_0 = 1.000×10^6) and medium system traffic

**Figure 6-19:** Constellation cost comparison for smallest contribution of fixed cost (k_0 = 1.000×10^3) and high system traffic

Figure 6-20: Constellation cost comparison for medium contribution of fixed cost ($k_0 = 5.000 \times 10^5$) and high system traffic

Figure 6-21: Constellation cost comparison for largest contribution of fixed cost ($k_0 = 1.000 \times 10^6$) and high system traffic

Chapter 7

Conclusions and Future Research

By examining the cost analyses, we can readily see that the GEO constellation proves to be the most cost-effective solution for supporting the projected space-borne user requirements. Its cost advantage over the MEO and LEO constellations is especially pronounced in situations of low and medium traffic. In these situation, the GEO constellation's advantage over MEO and LEO grows as the number of users increases. This is mainly because the GEO backbone is the most cost effective in supporting the user-access links, as can be seen in the previous section. Of the three constellations, GEO's most efficient aperture distribution leads to the least number of wasted and excessive apertures, causing its user-access link cost to be significantly less than other backbone constellations. This cost dominates in situations of light-to-medium overall system traffic, causing the GEO system to be the most cost-effective in those situations regardless of the relative efficiencies of the intra-backbone links.

The situation becomes a bit more complicated as the overall system traffic nears the upper limit of our projections. As system traffic increases, the cost of the intra-backbone links becomes more significant in the total cost, thus we must first analyze the cost of these links in each backbone before we can explain the overall system cost. From the plots of section 6.4.2, it is clear the LEO intra-backbone links have the most fixed cost but the least sensitivity to increased traffic, since they are able to divide the traffic over more possible paths. In contrast, GEO intra-backbone links have much smaller fixed cost than their LEO counterparts but are much more susceptible to cost increase due to increased system traffic. In situations of low traffic, cost does not grow as quickly with increased number of users, thus GEO intra-backbone links actually are less costly than LEO if the projected fixed cost is high (coefficient set 3). This reinforces the advantage of GEO is low traffic situations, although the contribution of intra-backbone link cost to overall cost is minute in this case. GEO's advantage is wiped out as projected overall system traffic approaches the upper limit of our projections, however. In this situation,

the GEO backbone link cost quickly increases with the number of users, while the LEO cost remains relatively constant. Thus, for greater than 20 users, the GEO backbone link cost exceeds the LEO cost. Since backbone link cost is a significant portion of the overall system cost in this range, the overall cost advantage of the GEO backbone virtually disappears as the number of users increases. It is very foreseeable that future demands increased of data-rate capacity or increased number of users could render LEO or MEO the more attractive backbone constellation due to their advantage in intra-backbone link cost and their better scalability to increasing number of users. Still, for a majority of the range of present projections, GEO is the most cost effective constellation. And for the small portion of circumstances where it does cost more than another constellation, such as for a range of users under high traffic assumptions, its cost remains very close to that of the leading constellation, LEO.

The analysis also proved to be fairly consistent no matter whether fixed cost played a great or small role in total link cost. For user-access links, the large number of users likely ensured that sheer aperture quantity played a more significant role in determining cost than either the fixed or variable costs of an individual aperture. For backbone links, the contribution of fixed cost did make a difference at low levels of system traffic, but, as previously noted, low system traffic also reduced the contribution of intra-backbone link cost to the cost of the entire system, thus we were unable to note any significant effect of fixed versus variable cost on the final system cost analysis.

Outside of cost analysis, the GEO constellation may also prove advantageous over other constellations for reliability and simplicity reasons. It is a well understood orbit with a large body of already existing satellites and associated knowledge. Its geo-stationarity is an advantage for terrestrial users, and the fact that it is also stationary with respect to GEO users could allow service via essentially fixed apertures, resulting in potential power savings. Thus, selecting GEO constellation as a space data-backbone would not be an imprudent choice, with the only cause for second thought coming in situations of high traffic, high user-count, and low-to-medium fixed cost, where LEO might be a better option.

Several potential research directions result from this work. One essential area of research which should be pursued is the effect of downlinks on system cost and performance. While the space data backbone network mainly services orbiting users, many of the data streams do terminate at a sink on the ground. Thus, downlinks are a significant factor in the design of the system. It would be a worthy effort to pursue how downlinks affect the performance of the particular backbones. Another potential area for research is the application of more optimal routing algorithms to the constellations coupled with a more realistic modeling of traffic to see if required cross-link capacities could be reduced. Other research directions would extend the status of the backbone network beyond its current state, as an conceptual exploration into the suitability of various backbone constellations, into a more realized design.

References

[1] Vincent W. S. Chan, "Optical Space Communications." *IEEE Journal on Selected Topics in Quantum Electronics Vol. 6, No. 6, Nov/Dec, 2000 –LEOS Millennium Issue.*

[2]   J. G. Walker, "Satellite Constellations." *Journal of the British Interplanetary Society. Vol 37, pp. 559-571, 1984.*

[3] J. G. Walker, "Continuous Whole-Earth Coverage by Circular Orbit Satellites." *Satellite Systems for Mobile Communications and Surveillance.* IEE Conference Publication 95, 35-38, 1973.

[4] National Aeronautics and Astronautics Administration. AP8max and AE8max trapped particle models. *http://nssdc.gsfc.nasa.gov/space/model/models/trap.html.*

[5] Analytical Graphics, Inc. *Satellite Tool Kit version 4.2.0.* 325 Technology Drive, Malvern, PA. ©1989-2000.

[6] Kenneth C. H. Kwok, *Cost Optimization and Routing for Satellite Network Constellations*, S.M. Thesis, Massachusetts Institute of Technology, Department of Electrical Engineering and Computer Science, February 2001.

[7] National Aeronautics and Astronautics Administration. Cost Estimating Group. "US Expendable Launch Vehicle Data for Planetary Missions." http://www.jsc.nasa.gov/bu2/ELV_US.html.

[8] Cyrus Jilla. *A Multidisciplinary Design Optimization Methodology for Distributed Satellite Systems.* Ph.D. Dissertation Proposal. Massachusetts Institute of Technology, Department of Aeronautic and Astronautic Engineering.

[9] Todd Mosher, M. Barrea, D. Bearden, and N. Lao, "Integration of Small Satellite Cost and Design Models for Improved Conceptual Design-to-Cost." *IEEE Aerospace Conference Proceedings, March 21-28, 1998, Vol. 3*, pp 97-103.

[10] John V. Evans, "Satellite Systems for Personal Communications." *Proceedings of the IEEE, Vol. 86, No. 7, July 1998*, pp 1325-1341.

[11] Markus Werner, A. Jahn, E. Lutz, and A Bottcher, "Analysis of System Parameters for LEO/ICO-Satellite Communication Networks." *IEEE Journal on Selected Areas in Communications, Vol. 13, No. 2, February 1995*, pp. 371-381.

[12] NASA Mission Services Program Office, "Space Network Overview." Reference at http://nmsp.gsfc.nasa.gov/tdrss/present.htm.